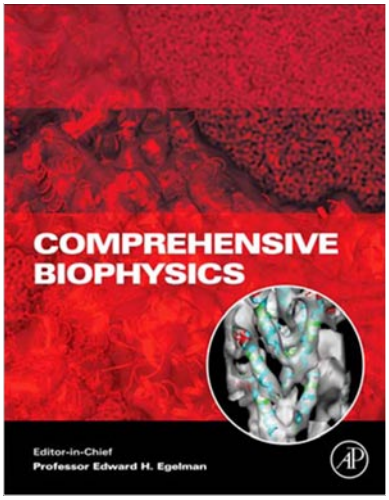

From D. Wirtz, Biophysics of Molecular Cell Mechanics. In: Edward H. Egelman, editor: Comprehensive Biophysics, Vol 7, Cell Biophysics, Denis Wirtz. Oxford: Academic Press, 2012. pp. 104-121.
ISBN: 978-0-12-374920-8

7.8 Biophysics of Molecular Cell Mechanics

D Wirtz, Johns Hopkins University, Baltimore, MD, USA

Abbreviations

3-D three-dimensional
AFM atomic force microscopy
GFP green fluorescence protein
LINC linkers of nucleus and cytoskeleton
MSD mean squared displacement
VEGF vascular endothelial growth factor

Glossary

Creep compliance The time-dependent deformation induced by continuously applied stress. Compliance is proportional to time and inversely proportional to viscosity for a viscous liquid. Compliance is independent of time for an elastic solid. Time-dependence of creep compliance of cytoplasm and nucleus is hybrid between those of a liquid and a solid. Creep compliance is dimensionless.

Elasticity Quantity that measures the propensity of a material to rebound after a deformation is eliminated. It is also called storage, stiffness, or elastic modulus. The elasticity of a material typically depends on both the amplitude and the rate of the applied deformation. Elasticity is expressed in units of $Pa = N\ m^{-2}$ or $dyn\ cm^{-2}$. See typical values in **Tables 1** and **2**.

Strain The shear deformation experienced by a material; it is either externally applied or induced in the material by an applied mechanical stress. Strain is dimensionless.

Stress The force per unit area to which a material may be subjected; it is either externally applied or induced in the material by an applied mechanical strain. Stress is proportional to strain for an elastic solid, and is proportional to the rate of strain for a viscous liquid. Stress is expressed in units of Pa.

Viscosity Quantity that measures the propensity of a material to flow. It is the ratio of the stress over the rate of deformation. Viscosity is expressed in units of $Pa \times s$. See typical values in **Tables 1** and **2**.

7.8.1 Introduction and Motivation

A multitude of cellular functions in both normal and pathological conditions depend critically on the dynamic changes in the mechanical compliance of the cytoplasm and nucleus, and the cell as a whole. For example, migrating epithelial cells at the wound edge significantly increase the elasticity of their cytoplasm so to produce net forces by actin filament assembling against the plasma membrane at the protruding cellular edge.[1,2] In migrating cells, the regulated movements of the nucleus, which is very stiff, within the cytoplasm, which is much softer, is partly controlled by the local viscosity of the cytoplasm.[3–6] The organization of chromosomes depend on the local micromechanical properties of the intranuclear space, which mechanically softens in laminopathies and following oncogenic transformation. Cells derived from mouse models of progeria (premature aging) or muscular dystrophy display significantly softer (i.e., less elastic) cytoplasm than

 doi:10.1016/B978-0-12-374920-8.00708-6

their wild-type controls,[3] which in turn affects these cells' ability to resist shear forces and migrate during wound healing processes.[7]

The method of particle tracking microrheology, which was introduced more than 15 years ago,[8] allows for rapid measurements (~30 s) of the local viscoelastic properties of the cytoplasm and nucleus in live cells *in vitro* and *in vivo*.[9] In this method, the spontaneous movements of submicron fluorescent beads dispersed throughout the cytoplasm and/or the nucleus of live cells (**Figure 1**) are monitored by time-lapsed fluorescence microscopy.[8] Movements of multiple beads are recorded simultaneously with a spatial resolution < 10 nm by tracking the beads' centroids. The recorded movements of the beads are transformed into mean squared displacements, which can subsequently be analyzed in terms of local, frequency-dependent, viscous and elastic moduli of the cytoplasm and nucleus. Particle tracking microrheology has been successfully used to probe the viscoelastic properties of various types of cells in a wide range of normal and disease conditions.[7,10–21] These measurements have revealed important new mechanistic insights into the biophysical mechanisms by which the micromechanical properties of the cytoplasm and nucleus adapt to various chemical and physical stimuli, how they can control key cell functions – such as cell division, cell migration, and cell polarization; and how these micromechanical properties are often altered in the context of disease, including cancer, muscular dystrophy, and progeria.

This chapter describes the basic concepts of mechanics and polymer physics that form the foundations of particle tracking microrheology. We also describe the key advantages of particle tracking microrheology over traditional cell-mechanics methods in a wide range of applications. This review then shows how particle tracking microrheology can readily reveal the lost ability of a wide range of diseased cells to deform and resist shear forces.

7.8.2 Basic Concepts of Molecular and Cellular Mechanics

7.8.2.1 Definitions of Stress, Strain, Viscosity, Elasticity, and Compliance

Because different experimental methods measure different rheological parameters, the intracellular mechanics of a living cell is best characterized by multiple, and often related, rheological quantities, including viscosity, elasticity, and creep compliance. These rheological parameters describe in different ways the mechanical response of a material (such as the cell's cytoplasm or the intranuclear network) subjected to a force or

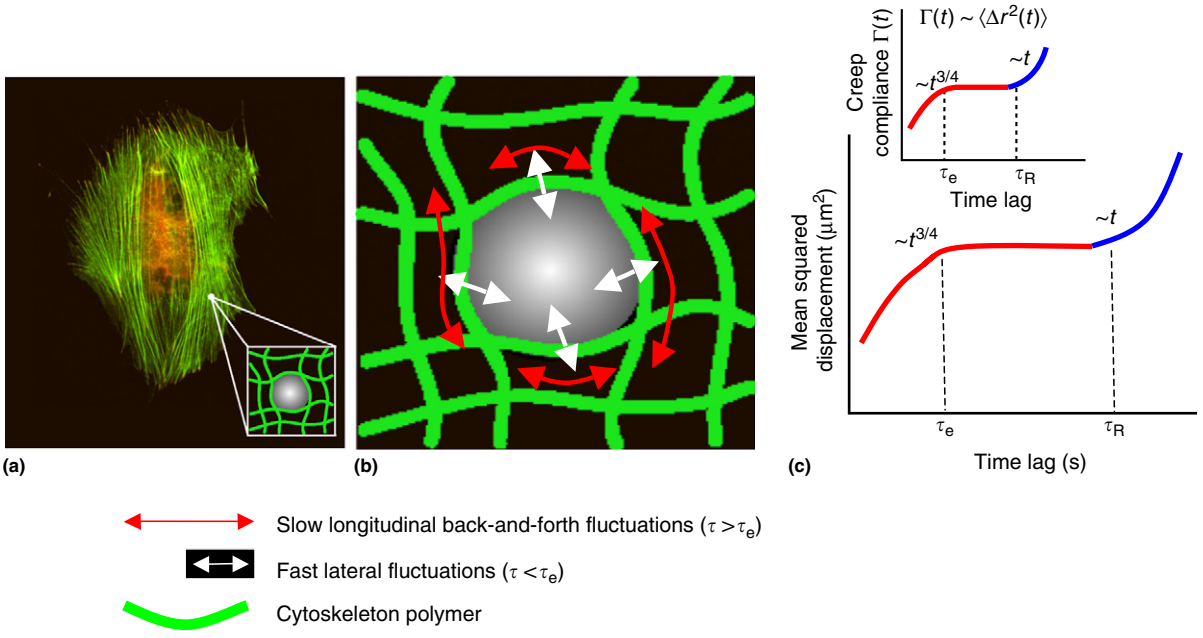

Figure 1 Particle tracking microrheology. (a) Submicron fluorescent beads are dialyzed and placed inside a ballistic injection machine. After ballistic injection, the beads disperse rapidly within the cytoplasm. The cells are placed under a high-magnification fluorescence microscope. Ballistically injected beads are lodged within the cytoskeleton. The size of the beads is chosen to be larger than the average mesh size of the cytoskeleton network, ~50 nm in fibroblasts. (b) The spontaneous movements of the cytoskeleton filaments that surround each bead induce displacements of the beads. At short timescales, the displacements of the beads are predominantly induced by the fast lateral bending fluctuations of the cytoskeleton filaments (white arrows). At long times, the displacements of the beads are predominantly induced by the slow longitudinal back-and-forth lateral fluctuations of the cytoskeleton filaments (red arrows). Finally, filaments move sufficiently to allow beads to escape the cage to move to the next cage. (c) Accordingly, the mean squared displacements of the beads show a $t^{3/4}$ power-law dependence at short timescales, a quasi-plateau value at intermediate timescales between τ_e and τ_R, and a linear dependence at long times caused by the slow viscous diffusion of the beads. Inset: The time lag-dependent mean squared displacements of the beads are subsequently transformed into local values of the creep compliance, $\Gamma(t)$, of the cytoplasm. Taken from Panorchan, P.; Lee, J. S.; Daniels, B. R.; Kole, T. P.; Tseng, Y.; Wirtz, D. Probing cellular mechanical responses to stimuli using ballistic intracellular nanorheology. *Methods Cell Biol.* **2007**, *83*, 115–140.

mechanical stress and measuring the resulting deformation or, vice versa, subjected to a deformation and measuring the force or stress that is required to produce the deformation. As discussed in detail below, the rheological response of the cytoplasm can be either predominantly viscous or elastic, depending on the time of application, the magnitude of the applied stress, and genetic/pharmacological manipulations of the cells. These forces can be externally applied as in the case of endothelial cells subjected to hemodynamic flow,[10] result from internal tension as in the case actomyosin contractility, or both.[22]

The shear viscosity of a liquid measures its propensity to flow when this liquid is subjected to a constant force. The shear viscosity induces the viscous drag that resists the motion of organelles and protein complexes in the cytoplasm and nucleus of cells. A simple way to measure the viscosity of a liquid *ex vivo* is to use a falling-ball viscometer. Here the speed at which heavy balls fall through the probed liquid depends on an effective viscosity of the liquid. This method is highly approximate due to the uncontrolled interactions between the balls and the suspending liquid and the inherent difficulty in measuring the terminal velocity of the falling balls precisely. Alternatively, the liquid can be subjected to a steady shear deformation of controlled rate using a rheometer. Here, the liquid is placed either between two parallel plates or between a cone and a plate, which maintains a constant shear rate. The viscosity is the ratio of the output stress (force per unit area) induced in the liquid by the input shear deformation to the rate of deformation. In cells, the interstitial viscosity, corresponding to length scales smaller than the mesh size of the cytoskeleton, controls the motion of globular proteins, while the mesoscale viscosity of the cytoplasm, corresponding to length scales larger than the mesh size of the cytoskeleton of the cytoplasm, predominantly governs the random movements and directed transport of organelles and cytoskeleton structures at long timescales.

A material that is only viscous (and not elastic), for example, water or glycerol, cannot resist mechanical stresses, it can only slow down its deformation by the imposed mechanical stress. Upon cessation of the stress, flow stops instantaneously and the material or liquid has lost all memory of its original shape and location. A classical illustration of this phenomenon consists in subjecting a (transparent) viscous liquid contained in a cylinder in which a droplet of black ink is deposited and subjected to a rotation for a couple of turns. Following concentric flow lines, the droplet elongates. Upon reversal of the rotational movement of the cylinder, the deformed droplet can be returned to its original shape, as long as diffusive dispersion of the ink particles has not occurred. Below, we will show how the viscosity of a liquid can be obtained by tracking the random movements of submicron beads embedded in the material of interest. The units describing the viscosity of a liquid are those of a force per unit time multiplied by time, $(N \times s)\ m^{-2}$ or Pa.s or Poise (1 Pa.s = 10 Poise). Examples of values of viscosity are given in **Tables 1** and **2**.

The elasticity (also called the elastic modulus or stiffness) of a material measures its stretchiness. Elasticity measures the ability of cytoplasmic structures to resist forces and store energy caused by deformation stemming from external or internal forces. A material that is only elastic (and not viscous) can deform under stress, but cannot flow. A material of high elastic modulus deforms less than a material of low elastic modulus when both are subjected to the same force. As no viscous dissipation occurs during deformation, an elastic material snaps back to its original shape upon cessation of the stress. Unlike cytoplasmic viscosity, cytoplasmic elasticity typically governs the rheological response of the cytoplasm to mechanical stresses at short timescales. The units describing the elasticity or elastic modulus of a material are $N\ m^{-2}$ or Pa (in the MKS unit system) or dyn cm^{-2} (in the CGS unit system), that is, the elasticity has dimensions of a force per unit area or pressure.

Some materials, such as silly putty, are both viscous and elastic. Silly putty can bounce as it deforms upon impact, but quickly regains its shape, which indicates it is elastic. It is also viscous, as silly putty rolled into a ball will partially flatten due to its own weight when left on a surface. Hence silly putty is predominantly elastic at short timescales (i.e., during impact), and predominantly viscous at long timescales (i.e., during spreading). Similarly, the cytoplasm of living cells is viscous at long timescales and elastic at short times scales, that is, the cytoplasm is viscoelastic.

Instead of working in the temporal domain, rheologists tend to work in the frequency domain. The frequency-dependent elastic modulus of a material, $G'(\omega)$, can be obtained by subjecting the material to oscillatory deformations of increasing frequency ω and constant (small) amplitude and measuring the resulting frequency-dependent stress induced in the material. This can be achieved using a strain-controlled rheometer. Moduli can also be obtained by subjecting a material to frequency-dependent stresses and measuring the resulting deformation. This can be achieved using a stress-controlled rheometer. Consider an oscillatory deformation given by the time-dependent function $\gamma(t) = \gamma_0 \sin\omega t$; then the stress, τ, induced by this deformation within the material will also be oscillatory, but will typically have both sine and cosine components. Specifically, the output stress can be decomposed into a sine component, which is in-phase with the input deformation $\gamma(t)$, and a cosine component, which is out-of-phase with the input deformation:

$$\tau(t) = \tau' \sin\omega t + \tau'' \cos\omega t \qquad [1]$$

τ' and τ'' are simply the magnitudes of these two contributions. To define elastic and viscous moduli of the material, G' and G'', we now rewrite this last expression by placing the magnitude of the input oscillatory deformation, γ_0, as a prefactor:

$$\tau(t) = \gamma_0 (G' \sin\omega t + G'' \cos\omega t) \qquad [2]$$

This relationship defines the elastic modulus of the material, G', as equal to the in-phase component of the frequency-dependent stress τ' divided by the amplitude of the oscillatory deformation γ_0, that is,

$$G'(\omega) = \tau'/\gamma_0 \qquad [3]$$

Similarly, the viscous modulus (also called loss modulus) of the same material, $G''(\omega)$, can be obtained during the same

Table 1 Elasticity and shear viscosity of the cytoplasm of different types of cells measured by particle tracking microrheology

	Average viscosity (Poise)	*Average elasticity at 1 Hz (dyne cm^{-2})*	*References*
Serum-starved Swiss 3T3 fibroblast[a]	10 ± 3	50 ± 20	22
Serum-starved Swiss 3T3 fibroblast treated with LPA[b]	95 ± 20	120 ± 30	22
Serum-starved Swiss 3T3 fibroblast subjected to shear flow[c]	300 ± 40	600 ± 50	10
Swiss 3T3 fibroblast at the edge of a wound[d]	45 ± 15	330 ± 30	1
Swiss 3T3 fibroblast treated with bradykinin[e]	22 ± 13	90 ± 20	1
Swiss 3T3 fibroblast treated with PDGF[f]	24 ± 8	190 ± 30	1
Mouse embryonic fibroblast ($Lmna^{+/+}$ MEF)[g]	18 ± 2	140 ± 30	7
MEF treated with latrunculin B[h]	NA	80 ± 4	7
MEF treated with nocodazole[i]	NA	50 ± 4	7
MEF deficient in lamin A/C ($Lmna^{-/-}$ MEF)	8 ± 1	60 ± 4	7
HUVEC cell on a planar 2-D peptide matrix[j]	17 ± 1	130 ± 10	PP, JSHL, DW, unpublished
HUVEC cell on a planar 2-D peptide matrix and treated with VEGF[k]	8 ± 1	100 ± 5	PP, JSHL, DW, unpublished
HUVEC inside a 3-D peptide matrix[j]	14 ± 1	55 ± 4	110
HUVEC inside a 3-D peptide matrix treated with VEGF[k]	18 ± 1	40 ± 3	110
HUVEC inside a 3-D fibronectin matrix	NA	58 ± 6	111
HUVEC inside a 3-D fibronectin matrix treated with inhibiting FN peptide	NA	20 ± 4	111
Single-cell *C. Elegans* embryo[l]	10 ± 1	negligible	92
Interphase nucleus of Swiss 3T3 fibroblast[m]	520 ± 50	180 ± 30	12

[a]Cells placed on 50 $\mu g\ ml^{-1}$ fibronectin-coated glass were serum starved for 48 h before measurements.
[b]Serum-strarved cells placed on 50 $\mu g\ ml^{-1}$ fibronectin-coated glass were treated with 1 $\mu g\ ml^{-1}$ lysophosphatidic acid (LPA), which activates Rho-mediated acto-myosin contractility. LPA was applied 15 min before measurements.
[c]Cells were grown 20 $\mu g\ ml^{-1}$ fibronectin-coated glass substrate for 24 h and exposed to shear flow (wall shear stress, 9.4 dynes cm^{-2}) for 40 min before measurements.
[d]Cells in complete medium and grown on 50 $\mu g\ ml^{-1}$ fibronectin-coated glass substrate to confluence were wounded to induce migration. Measurements were conducted 4 h after wounding.
[e]Cells in complete medium and grown on 50 $\mu g\ ml^{-1}$ fibronectin-coated glass substrate were treated with 100 $ng\ ml^{-1}$ bradykinin for 10 min before measurements.
[f]Cells in complete medium and grown on 50 $\mu g\ ml^{-1}$ fibronectin-coated glass substrate were treated with 10 $ng\ ml^{-1}$ PDGF for 10 min before measurements.
[g]Cells in complete medium were grown on glass.
[h]$Lmna^{+/+}$ MEFs in complete medium grown on glass were treated with 5 $\mu g\ ml^{-1}$ actin-filament disassembly drug latrunculin B.
[i]$Lmna^{+/+}$ MEFs in complete medium and grown on glass were treated with 5 $\mu g\ ml^{-1}$ microtubule-disassembly drug nocodazole.
[j]Cells in complete medium were placed in a 0.5% puramatrix gel.
[k]Cells in complete medium were placed in a 0.5% puramatrix gel and treated with 4 $ng\ ml^{-1}$ VEGF for 24 h prior to the measurements.
[l]Young *C. elegans* eggs were obtained by cutting gravid hermaphrodites from worms in egg salts. The nanoparticles were then microinjected into the syncytial gonads of gravid hermaphrodites.
[m]Cells in complete medium.

Particle tracking microrheology measurements of shear viscosity and elasticity of a wide range of cells. Unless stated, all values of viscosity and elasticity in the table are for the cytoplasm. The elasticity was evaluated at a shear frequency of 1 s^{-1} (1 $s^{-1} = 1$ Hz) and the shear viscosity was estimated as the product of plateau modulus and the relaxation time. The plateau modulus is the value of the elastic modulus where it reaches a quasi plateau value at intermediate frequencies. The relaxation time is the inverse of the frequency where elastic and viscous moduli are equal. All measurements are mean $\pm$ sem. Unit conversions are 1 dyne $cm^{-2} = 0.1$ Pa $= 0.1$ N $m^{-2} = 0.1$ pN μm^{-2}. Pa, Pascal; pN, piconewton; NA, not available.

From Wirtz, D. Particle-tracking microrheology of living cells: principles and applications. *Annu. Rev. Biophys.* **2009**, *38*, 301–326. Copyright by Annual Reviews.

measurement by extracting the out-of-phase component of the frequency-dependent stress τ'' and divide by the amplitude of the oscillatory deformation γ_0,[23] that is

$$G''(\omega) = \tau''/\gamma_0 \quad [4]$$

If applied deformations are sufficiently small, the stress is linearly dependent on the magnitude of the imposed deformation (eqn [2]) and moduli G′ and G″ are independent of the amplitude of deformation γ_0. This is the so-called linear regime for which stress and strain are proportional to each other. At larger deformations, the cell and networks of cytoskeleton networks will feature moduli that depend on the amplitude of deformation. This is the nonlinear regime of deformation for which stress and strain are not proportional to each other anymore. For instance, an entangled network of actin filaments *in vitro* will show a constant elasticity independent of strain at very low strain amplitudes (<2%; the linear regime), will strain-harden (G′ increases for increasing deformation; the beginning of the nonlinear regime) for intermediate deformation amplitudes, and will strain-soften (G′ decreases for increasing deformation) for large deformation amplitudes.[24] This biphasic behavior for G′ represents the nonlinear regime for which moduli depend on the amplitude of deformation. Many biopolymers display strain-hardening behavior.[25]

Let us now consider the two limit cases of a purely viscous liquid and of a purely elastic solid. If the material is an elastic solid (showing no measureable viscosity), such as rubber or concrete, then the stress induced by deformation is exactly in

Table 2 Viscosity and elasticity of common liquids and cytoskeletal filament networks measured by a cone-and-plate rheometer

	Average viscosity (Poise)	*Average elasticity at 1 rad s^{-1} (dyne cm^{-2})*	*References*
Water	0.01	0	
Blood	0.1	negligible	
Glycerol	~1	negligible	
Corn syrup	~20	negligible	
Ketchup	~500	negligible	
Jello	negligible	1000	
Polyacrylamide gel		500	112
F-actin network		8±3	24
F-actin + filamin		450±60	45
F-actin + α-actinin		120±20	24
F-actin + Arp2/3 complex/WASp		60±15	113
F-actin + fascin		80±10	114
F-actin + fimbrin		300±30	115
Vimentin network		14±2	116

Measurements are mean±sem. The elasticity was measured at a shear amplitude of 1% and a shear frequency of 1 rad s^{-1}. Shear viscosity of the F-actin and vimentin networks was not measured because these filaments break under continuous shear.

The concentrations of actin and vimentin solutions are 24 μM. The concentrations of α-actinin, fascin, fimbrin, and filamin in solutions are 0.24 μM. The concentration of Arp2/3 complex is 0.12 μM and that of its activator WASp is 0.06 μM. The concentration of acrylamide and bis-acrylamide in the polyacrylamide gel is 0.04% and 0.05%, respectively. Unit conversions are 1 Poise = 0.1 Pa s; 1 dyne cm^{-2} = 0.1 Pa.

From Wirtz, D. Particle-tracking microrheology of living cells: principles and applications. *Annu. Rev. Biophys.* **2009**, *38*, 301–326. Copyright by Annual Reviews.

phase with the input deformation and $\tau(t) = \tau' \sin\omega t$. In this case, the viscous modulus is vanishing low, $G'' = 0$ and $G' \neq 0$. In contrast, if the material is a viscous liquid (no measureable elasticity), such as water or glycerol, then the output stress is out of phase with the input deformation, and $\tau(t) = \tau'' \cos\omega t$. In this case, the elastic modulus is vanishingly low, $G' = 0$ and $G'' \neq 0$.

In addition to dependence on the magnitude of deformation, typical biomaterials, such as living cells and tissues, have rheological properties that depend on the rate of the imposed deformation, ω, that is, the moduli G' and G'' both depend on ω. By definition, a material that is more viscous than elastic, that is $G''(\omega) > G'(\omega)$, is a viscoelastic liquid at least over a certain range of frequencies; a material that is more elastic than viscous, $G'(\omega) > G''(\omega)$, is a viscoelastic solid. At low deformation frequencies, the cytoplasm has the time to reorganize its cytoskeleton polymers and it can flow, behaving mostly as a viscous liquid showing little elasticity, that is, the cytoplasm is a viscoelastic liquid at low frequencies. At high deformation frequencies, the cytoplasm does not have the time to reorganize and relax the imposed stress and the cytoplasm behaves as an elastic solid, which resists the deformation, that is, the cytoplasm is a viscoelastic solid at high frequencies. This example illustrates the importance of measuring the full frequency-dependent response of cells and tissues, which undergo both slow and rapid movements depending on physiopathological conditions, as opposed to a single-valued elasticity and viscosity. Unlike particle tracking microrheology, most cell-mechanics approaches cannot measure frequency-dependent moduli, which is a severe limitation.

The rheology of individual cells cannot be measured with a macroscopic device, such as the rheometer used routinely to measure the viscoelastic properties of complex fluids. Moreover, even if a micron-scale rheometer existed, measuring the full frequency-dependent rheological response of the cytoplasm to oscillatory deformations would be extremely tedious, as this response would have to be probed one frequency at a time over a wide range of frequencies. Below, we will show that the frequency-dependent viscous and elastic moduli of a cell can be measured by monitoring the spontaneous movements of sub-micron beads embedded in the cytoplasm or nucleus of a cell, without subjecting the cell to any external force or deformation.

Finally, the creep compliance of the cytoplasm, Γ, refers to its deformability. A high compliance indicates that a material has a low propensity to resist mechanical deformation as it is being subjected to a shear stress; a low compliance indicates that it can resist such mechanical stress. Experimentally, it is measured as the time-dependent deformation of the cytoplasm resulting from a continuously applied mechanical stress (applied force per unit area). When the material is only viscous (i.e., it is a liquid), then its time-dependent creep compliance increases linearly with the duration of stress application and is inversely proportional to the viscosity of the liquid. Vice versa, when a material is only elastic, then its creep compliance is independent of time and is inversely proportional to the elasticity of the material. Below, we will show how the time-dependent creep compliance of the cytoplasm can be obtained directly from tracking the movements of the centroids of submicron beads in the cytoplasm. Indeed, the time-dependent creep compliance, $\Gamma(t)$, is directly proportional to the mean squared displacement of the cytoplasm-embedded bead.

Importantly, the rheological parameters described above are related to one another. Viscoelastic moduli G' and G'' and compliance $\Gamma(t)$ of the cytoplasm are mathematically related to one another. Indeed, it is possible to compute the time-dependent cytoplasmic creep compliance from the frequency-dependent viscoelastic parameters through integration and, vice versa, the viscoelastic moduli of the cytoplasm can be computed from the time-dependent creep compliance. The shear viscosity can also be estimated from the frequency-

dependent viscous and elastic moduli and from the product of the relaxation time and plateau modulus of the cytoplasm, defined in more detail below. Finally, at high frequencies ($\omega > 1$ kHz), due to Kramers-Kronig relations, viscoelastic moduli G′ and G″ become proportional to one another.[26]

7.8.2.2 A Model System: A Solution of Actin Filaments

To gain an intuitive understanding of the rheological definitions given in the precedent section, we consider the relatively simple system of a concentrated solution of actin filaments suspended in buffer. Along with microtubules and intermediate filaments, F-actin is one of three major filamentous proteins of the cytoskeleton, providing it with the largest contribution to cytoplasmic stiffness, which in turn provides the cell with its structure and shape.[19] In the cytoplasm of all cell types, actin monomers (G-actin) assemble into F-actin. F-actin is a semiflexible polymer since its persistence length, a measure of the filament's bending rigidity, is similar to the filament's contour length, both ~ 15 μm *in vitro*. In contrast, intermediate filaments and DNA are more flexible polymers than F-actin, while microtubule is a more rigid polymer than F-actin, at least *in vitro*, with a persistence length approximately equal to 1 mm. Because it is a semiflexible polymer, F-actin can readily form networks that are entangled even at low concentrations.[27–29] These entanglements limit the lateral motion of the polymers in the network and, in turn, cause the elasticity of the network. In contrast, flexible polymers can only form an elastic network at high concentrations. The viscoelastic properties of F-actin networks can be controlled *in vitro* by either altering the concentration of F-actin or the concentrations of F-actin crosslinking/bundling proteins, such as α-actinin or filamin, or both.[24,30]

As noted above, the cytoplasm of adherent cells (i.e., not suspension cells like blood cells) is rheologically complex. Cytoplasm typically behaves as a viscoelastic liquid when either sheared slowly or for a long time, and as a viscoelastic solid when either sheared rapidly or for a short time. This rheological complexity can be partially recapitulated using a solution of entangled actin filaments assembled with purified actin and the motor protein myosin II or a crosslinking proteins such as α-actinin.[31,32] Below a threshold concentration of approximately 0.1 mg/ml, actin filaments cannot form an entangled network and, as a result, cannot resist shear deformations. The rheological response of this actin solution is viscous at all probed timescales, with a viscosity equal to that of buffer with a correction due to the presence of the filaments.[33] However, beyond this threshold concentration, actin filaments in suspension begin to form entanglements. These entanglements form topological obstacles for polymer motion within the network, which causes the elasticity of the network.

At short timescales, the filaments undergo random, lateral fluctuations (**Figure 1(b)**). These fluctuations are rapid since they involve the small sections of the filaments between network entanglements. A fast camera can readily show that a fluorescently labeled actin filament embedded in unlabeled filaments undergoes lateral fluctuations within a confining tube-like region formed by the surrounding filaments.[33–35] Scaling concepts, introduced by de Gennes can semiquantitatively predict describe this dynamics.[33] For timescales that are longer than the time required for the lateral fluctuations to begin to reach the tube-like region of the surrounding filaments, back-and-forth (random) longitudinal movements of the filament in the network take place (**Figure 1(b)**). Unlike lateral bending movements of the filaments, these longitudinal motions are slow because they involve the entire filament. At intermediate timescales, these back-and-forth, snake-like movements, also called reputation,[33] result in no net displacement of the filaments. The movements of the filaments resemble gently curved 'one-dimensional' random walks. At timescales longer than a characteristic 'terminal' relaxation time of the network, which strongly depends on the length of the filaments, the filament can finally escape the tube-like region.[36,37] At these long timescales, the polymer network behaves as a viscous liquid. Because actin filaments are long and rigid, this terminal relaxation time is extremely long and equal to tens of minutes.

The short- and long-timescale-dependent movements of individual filaments in a dense network can be described in rheological terms.[33] Consider an actin filament network subjected to a constant mechanical stress of relatively small magnitude. At short timescales, the filaments can only 'relax' the energetically unfavorable distortions created in the polymer network by the externally applied stress through lateral fluctuations.[36] At these short timescales, the creep compliance – that is, the deformation of the network caused by the applied stress – increases as a power law of time, as $t^{3/4}$ (Inset, **Figure 1(c)**).[38] The exponent $^3/_4$ reflects the lateral bending fluctuations of the filaments.[36,39] This exponent would be $^1/_2$ for flexible polymers, such as DNA. We note that this exponent is close to $^3/_4$ for the cytoplasm of fibroblasts,[26] further indicating that cytoplasmic rheology is dominated by actin filaments. Hence rheological measurements can reveal the bending rigidity of a polymer, if unknown.

At longer timescales, the network cannot relax anymore since no net filament motion occurs at these timescales as polymers are undergoing each reptation in tube-like regions created by surrounding polymers. Accordingly, the creep compliance of the filament network becomes approximately time-invariant, a constant called a 'plateau' (**Figure 1(c)**). At least at these intermediate timescales, the polymer network behaves mostly as an elastic gel. Here the elastic modulus becomes much larger than the viscous modulus. Although not physiological, a stably crosslinked actin filament network would also be more elastic than viscous, but at all timescales.[40] Finally, at long timescales, the test actin filament finally moves out of its confining tube-like region, the network can relax the imposed stress. The creep compliance (i.e., network deformation) starts growing linearly with time, a proportionality that reflects viscous behavior at long timescales.[41] The network becomes a viscoelastic liquid, for which the viscous modulus is much larger than the elastic modulus.[23] If the actin filament network were stably crosslinked, the polymer could not undergo this terminal relaxation and the plateau value of the compliance would persist indefinitely in a graph of creep compliance as a function of time. Often the transition from the plateau region at intermediate timescales to the terminal relaxation region at long timescales is not sharp. Rather the transition of broad and the compliance curve forms

a 'shoulder' because actin filaments in solution have a wide distribution of lengths, corresponding to a broad distribution of relaxation times. If one uses regulators of F-actin length distribution, then this shoulder becomes sharper.

A permanently crosslinked actin filament network would provide cells with structural stability, but would not allow them to mechanically soften to mediate cell shape changes that are, for instance, required during cell intravasation and extravasation steps of metastasis[42] and during migration of some cell subtypes in three-dimensional (3-D) stromal matrix.[43] Cells have evolved an ingenious mechanism to allow for both a stiff but malleable cytoskeleton. This mechanism does not require dynamic disassembly and reassembly of the filaments themselves to modulate the mechanical properties of the network. Rather, F-actin networks exploit dynamic crosslinking proteins, such as α-actinin or filamin,[42,44–46] which both dynamically bind F-actin and are present in different sections of the cell. α-Actinin crosslinks F-actin at stress fibers at the basal surface of the cell, while filamin crosslinks F-actin in the lamella. When an α-actinin- or filamin-crosslinked network is sheared more slowly than the lifetime of binding of α-actinin or filamin, the network can flow and it behaves mostly as a liquid. When sheared at a rate faster than the inverse binding lifetime of the crosslinking protein, the actin filament network behaves as an elastic gel and cannot flow.[42,44,47] Hence α-actinin and other dynamic crosslinking/bundling proteins would mediate mechanically 'auto-regulated' movements of cells.

At high concentrations of actin crosslinking proteins α-actinin and filamin or myosin II, these proteins mediate bundling of filaments *in vitro*. Cells display such actin filament bundles at their basal surface (as stress fibers), as well as arcs on the dorsal side of the lamella, and thick contractile fibers on top of the nucleus, which form the perinuclear actin cap.[48] These different actin bundle structures play distinct functions in cell and nuclear shaping and in migration. Some F-actin-binding proteins only bundle and do not crosslink F-actin, including fascin, which is concentrated in the thin filopodial protrusions at the leading edge of migrating cells. The differential ability of fascin and α-actinin/filamin to bundle as opposed to crosslink actin filaments may depend on the distance between their two actin-binding domains. A short distance between the two actin-binding domains of these proteins (the case for filamin and α-actinin) promotes tight crosslinking of actin filaments, that is, their bundling. In contrast, a large distance between the actin-binding domains of the protein promote actin filament bundling. As expected, F-actin bundling protein fascin does not increase the stiffness of a network as much as crosslinking proteins. This is because F-actin bundling alone, while fascin increases the stiffness of the building blocks of the network (i.e., the bundled filaments), it decreases their density in the network. Polymer physics predicts that stiffening of the polymers is much less potent than polymer density in increasing the elasticity of a polymer network. Computational modeling predictions, which were subsequently verified by experiments with purified proteins, suggest that combining a bundling protein (fascin) with a crosslinking protein (α-actinin) is significantly more effective at forming highly elastic F-actin networks than bundling proteins alone or crosslinking proteins alone for the same concentration of actin.[49,50] Rheology of F-actin networks *in vitro* also suggests that bona fide crosslinking proteins α-actinin and filamin do not play redundant rheological functions[49,50] and can form much stiffer actin filament network than any of these proteins alone at the same total concentration of crosslinking proteins.

7.8.3 Particle Tracking Microrheology

7.8.3.1 Particle Tracking Microrheology of a Viscous Liquid

Here we describe some of the basic principles of particle tracking microrheology. To understand how the viscoelastic properties of the cytoplasm or nucleus can be computed by tracking and analyzing the movements of submicron embedded beads, we consider first the simpler case of submicron beads suspended in a viscous liquid (no elasticity). These beads are chosen to be smaller than 1 μm so that they undergo Brownian motion, as inertial forces (gravity) are negligible. If active transport of the nanoparticles is also negligible (see more below), only two types of forces act on the beads inside the cytoplasm:

(i) The small random force produced by the random collisions of water molecules generated by the thermal energy k_BT (k_B is Boltzmann's constant, T is the absolute temperature) and the movements of other cytoplasmic structures, such as cytoskeleton filaments and other organelles.[8]
(ii) The counteracting frictional force that results from the movement of the beads driven by random forces. The frictional force is proportional to the velocity of the bead and the bead's friction coefficient, which depends on the viscoelastic properties of the cytoplasm and the size of the bead. It has all times the same magnitude as the random force and is points in the exact opposite direction.

Because we can neglect inertia and directed motion, the mathematical equation describing the motion of a bead simply states that the sum of these random and frictional forces is zero. The resulting equation is not deterministic but 'stochastic' (also called Langevin equation), because the force that drives the movements of the beads is itself random in amplitude and direction. The solution of this stochastic equation is the conventional random walk.[51] A probabilistic formulation of the random displacements of beads in a liquid is the Fokker-Planck equation. On average, a bead subjected to random and counteracting frictional forces remains at its initial position, that is, the first moment of the distribution is zero. However, the standard deviation of the displacements or the mean squared displacement (MSD) of the bead, $\langle \Delta r^2 \rangle$, is not zero, that is, the second moment of the distribution is not trivially zero.

Consider a liquid of (unknown) shear viscosity, η, in which a submicron bead has been suspended and, therefore, undergoes Brownian motion driven by the thermal energy k_BT. We aim at measuring η by tracking the movements of this bead. Each time the bead takes a step in a random direction (i.e., for each recorded frame of a movie), it loses all 'memory' of where it just came from (i.e., the previous frame) because the liquid is viscous and not elastic. For the next step (i.e., the next frame), the bead moves in a direction and with a

magnitude that are completely uncorrelated to the directions and magnitudes of the previous bead movements. Einstein showed that, in these conditions, the bead undergoes a random walk and its time-averaged MSD is simply (**Figure 2(a)**):

$$\langle \Delta r^2 \rangle = 4Dt \qquad [5]$$

In eqn [5], t is the time lag or timescale (the same timescale that we described in the previous section); the brackets $\langle \ldots \rangle$ indicate time-averaging over several moves of the bead; and D is the diffusion coefficient of the bead. The linear dependence of the MSD on timescale (eqn [1]) is indicative of viscous diffusion.[52] The square-root dependence of the root MSD with time, $\sqrt{\langle \Delta r^2 \rangle} = \sqrt{4Dt} \sim t^{1/2}$, is also indicative of viscous diffusion.[51] For a spherical bead, the diffusion coefficient is given by the relation $D = k_B T/\xi$, where $\xi = 6\pi\eta a$ is the Stokes–Einstein expression connecting the friction coefficient of the bead in the viscous liquid to the radius a of the bead and the viscosity of the liquid. To compute the unknown viscosity of the liquid from the measured movements of the bead, we can rearrange the previous expression. We obtain:[38]

$$\eta = \frac{2k_B T}{3\pi a} \frac{t}{\langle \Delta r^2(t) \rangle} \qquad [6]$$

This expression explains how one can estimate the viscosity of a liquid merely by submicron beads in that liquid and subsequently tracking their thermally-excited random motion using fluorescence light microscopy using an appropriate particle tracking software, and finally computing the MSD from the trajectories of the beads.

In practice, tens to hundreds of beads need to be tracked to ensure adequate statistics. In this case, the ensemble-averaged MSD, $\langle \Delta r^2(t) \rangle$, which is the average of all measured MSDs, is used instead of $\langle \Delta r^2 \rangle$. If the suspending fluid is indeed a liquid, then $t/\langle \Delta r^2(t) \rangle$ should be a constant independent of t (see eqn [1]), which is a stringent test of viscous diffusion. If $t/\langle \Delta r^2(t) \rangle$ is not constant, it usually indicates that the suspending fluid is a viscoelastic material instead of a viscous liquid, that is, it is both viscous and elastic.[53] If $t/\langle \Delta r^2(t) \rangle$ increased with t, then it is likely that the liquid moved during the experiments, presumably because of uncontrolled convection.

To illustrate the use of the above expressions, we now consider a 100 nm diameter bead suspended in corn syrup, which has a shear viscosity close to that of the cytoplasm of fibroblasts, $\eta = 20$ Poise $= 2$ Pa. s (typical values of viscosity are listed in **Tables 1** and **2**) and no elasticity. The thermal energy is $k_B T \approx 4.2$ pN.nm (where pN = piconewton and $T = 273.15 + 37\ ^\circ\text{C} = 310\ ^\circ\text{K}$ absolute temperature) and the diffusion coefficient of the bead is $D \approx 0.0022\ \mu\text{m}^2\ \text{s}^{-1}$ computed using the Stokes–Einstein relationship. By comparison, the diffusion of the same bead in water ($\eta = 0.01$ Poise) would be approximately $4.4\ \mu\text{m}^2\ \text{s}^{-1}$. Therefore, the value of the time-averaged MSD of the bead in corn syrup after times of 0.1 s, 1 s, and 10 s of tracking is respectively $\approx 0.00088\ \mu\text{m}^2$ (or 88 nm^2), 0.0088 μm^2, and 0.088 μm^2. These results indicate that the size of the regions encompassed by the Brownian movements of the bead after the same times is approximately $\sqrt{\langle \Delta r^2 \rangle} = \sqrt{4Dt} \approx 30$ nm, 94 nm, and 300 nm, respectively. Hence high-resolution tracking is required to obtain reliable measurements of the MSDs of 100 nm beads in a highly viscous liquid within a 10 s long tracking time. Alternatively, for a highly viscous liquid such as corn syrup, long-time tracking can be used to monitor displacements of beads so that they are sufficiently large that they can be more easily detected by light microscopy.

The prefactor 4 in the expression $\langle \Delta r^2 \rangle = 4Dt$ is due to standard light microscopy probing the two-dimensional projection of the three-dimensional movements of the bead. This prefactor is correct only if the probed material in the proximity of the bead is isotropic, that is, this material or liquid has the same physical properties in all 3 (x, y, and z) orthogonal directions. As an alternative to actual 3-D tracking of beads which can be achieved by tracking rings of diffraction,[54] and to test whether isotropy is likely to be correct for the material in question,[55] one can compute the MSDs of the bead in the x and y directions independently. From the time-dependent coordinates of the bead, $x(t)$ and $y(t)$, one obtains the total MSD of the bead defined as $\langle \Delta r^2(t) \rangle = \langle [x(t) - x(0)]^2 + [y(t) - y(0)]^2 \rangle$, where $x(0)$ and $y(0)$ are the initial

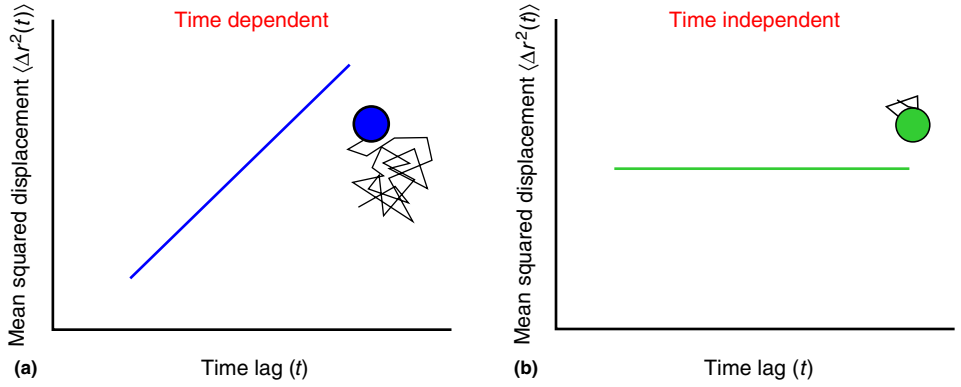

Figure 2 Particle tracking microrheology of a viscous liquid and an elastic solid. (a) The mean squared displacement of beads immersed in a viscous liquid (such as water or glycerol), grows linearly with time lag, with a slope inversely proportional to the viscosity of the liquid and the radius of the bead. (b) The mean squared displacement of beads embedded in an elastic solid liquid (such as rubber), is independent of time lag. The plateau value is inversely proportional to the elasticity of the solid. Adapted with permission from Wirtz, D. Particle-tracking microrheology of living cells: principles and applications. *Annu. Rev. Biophys.* **2009**, *38*, 301–326. Copyright by Annual Reviews.

position of the bead when starting tracking. If the probed material is isotropic, then $\langle [x(t)-x(0)]^2 \rangle = \langle [y(t)-y(0)]^2 \rangle$. Therefore, in this case, $\langle \Delta r^2(t) \rangle = 2\langle [x(t)-x(0)]^2 \rangle = \langle [y(t)-y(0)]^2 \rangle$. If the displacements of the bead in the x and y directions are indeed Brownian (i.e., x and y projections of the bead displacements are independent of each other and correspond both to one-dimensional random walks), then $\langle [x(t)-x(0)]^2 \rangle = \langle [y(t)-y(0)]^2 \rangle = 2Dt$. Therefore, $\langle \Delta r^2\ (t) \rangle = 4Dt$; if the last expression is experimentally verified, then the viscoelastic properties of the cytoplasm in the vicinity of the bead are likely to be isotropic.[56]

In the case of a viscous liquid, the elastic modulus of the liquid is negligible ($G' = 0$), and it can be shown that the viscous modulus is given by the product $G'' = \eta\omega$. Here, ω is the frequency (or rate) of the deformation in an oscillatory mode of deformation and is equal to the inverse of the time lag t, $\omega = 1/t$. This means that if this liquid were placed in a rheometer and subjected to oscillatory deformations, then the elastic modulus would be negligible and the viscous modulus would increase linearly with the input frequency ω. Equivalent to the linear dependence of the MSD with time, the fact that the viscous modulus of a given material increases linearly with ω is indicative that this material is a viscous liquid. This rheological response described by $G' \approx 0$ and $G'' = \eta\omega$, would be, for instance, that of an unpolymerized G-actin solution *in vitro* or that of the cytoplasm of a cell treated with a high concentration of an actin-depolymerizing drug.

If the probed system were perfectly uniform (same rheological properties everywhere), tracking one bead for a long time (say 1000 s) and dividing this time span, say, in 100 equal time spans of 10 s should be equivalent to tracking 100 beads each for 10 s. Although it is impractical to track a single bead for very long time periods, even in *in vitro* systems, because of drift problems and live cells, because of their movements, this equivalency is mathematically correct for liquids like water and glycerol, a signature of ergodicity. But it is incorrect in *in vitro* systems like actin filament suspensions and live cells, which are systems far from equilibrium and highly spatially heterogeneous.[57,58] Indeed, beads dispersed in the cytoplasm of an adherent cell typically show a wide distribution of MSDs.[8]

We note that individual trajectories of the beads, even in viscous liquids like water or glycerol, are asymmetric in shape.[56] Even the overall shape of a (single) computer-generated random walk is highly asymmetric,[51,59] that is, somewhat unexpectedly, it is not a circle. The shape of the object encompassing an individual trajectory of a single bead in a liquid is an ellipse in 2-D (e.g., the trajectory of a membrane protein in the plasma membrane) and is a completely asymmetric ellipsoid in 3-D (e.g., the trajectory of fluorescent protein such as GFP (green fluorescence protein) in the cytoplasm).[60] Of course, when these trajectories are ensemble-averaged and the trajectories are superimposed to one another, then the object encompassing these individual trajectories is a circle in 2-D and a sphere in 3-D.

7.8.3.2 Particle Tracking Microrheology of an Elastic Solid

The second example illustrating the basic principle of particle tracking microrheology involves a submicron bead embedded in an elastic material of negligible viscosity, such as rubber or concrete. Here, each time the bead is driven by the thermal energy in a random direction, the surrounding material instantaneously pushes back in the opposite direction with equal force. Therefore, the MSD of the bead is nonzero but constant: $\langle \Delta r^2 \rangle = C$, at all measured timescales (**Figure 2(b)**). An experimentally observed time-independence of the MSD is indicative of a purely elastic solid behavior. In this example, the viscous modulus of this solid is zero, $G''(\omega) = 0$. The elastic modulus of an elastic solid considered here is given by $G'(\omega) = 2k_BT/3\pi a\langle \Delta r^2 \rangle = 2k_BT/3\pi aC$, where C is a constant. This expression shows that $G'(\omega)$ is a constant independent of ω; moreover, it shows that the elastic modulus of an elastic solid is inversely proportional to the MSD of the beads embedded in it.

This example shows that one can compute the elastic modulus of an elastic solid from particle-tracking measurements of $\langle \Delta r^2 \rangle$ without imposing any oscillatory deformation to the material, but by tracking the spontaneous Brownian motion of beads serving as local physical probes of the material. When the elastic modulus of a given material is found to be independent of the rate of deformation, ω, it is indicative of its purely elastic behavior. This is the rheological response of a permanently crosslinked actin filament network[61] or Jello, for which G' is approximately a constant independent of frequency and G'' is much smaller than G'.

To estimate the viscosity of a liquid, a spatial resolution of at least 30 nm is required when tracking 100 nm diameter beads for 10 s using a camera collecting images at a rate of 10 frames per second. In practice, the spatial resolution on the displacements of the beads has to be an order of magnitude better, approximately 3 nm for a 100 nm diameter fluorescent bead. Such a high, subpixel spatial resolution can be obtained by either using quadrant detection or fluorescence video microscopy. The advantage of quadrant detection is its superior detection capability and spatial resolution (< 1 nm),[62] but quadrant detection can only track one or two beads at a time in the cytoplasm.[26,63,64] This is a serious problem when the viscoelastic properties of various locations within the cell need to be monitored simultaneously. With the use of high-magnification, high numerical-aperture lenses,[65] video microscopy can track 10–300 beads simultaneously,[8,66,67] but has a maximum resolution of the order of 1–10 nm. The spatial resolution of the measurements of bead displacements will vary from one instrument to another since spatial resolution also depends on the stability of the microscope system used to collect movies of beads. For an elastic material and with a spatial resolution of 3 nm, the highest elasticity that can be measured with accuracy using particle-tracking microrheology is approximately $G'_{max} = 2k_BT/3\pi a(3\ nm)^2 \approx 1900$ Pa $\approx$ 19 000 dyne/cm^2,[68,69] which is much higher than typical values of the elasticity of the cytoplasm, but too low for some very stiff biomaterials like bone.

7.8.3.3 Particle Tracking Microrheology of a Viscoelastic Material

Progressively moving towards more complex systems, we now describe the rheological behavior of the cytoplasm or a

reconstituted actin filament network. The rheological behavior of such systems is intermediate between the two above limit behaviors of a viscous liquid and an elastic solid. The cytoplasm is predominantly viscous at long timescales ($t > \tau_R$) or low rates of shear ($\omega < \omega_R$), $G''(\omega) \ll G'(\omega)$, and predominantly elastic at short timescales or high rates of shear, $G''(\omega) \gg G'(\omega)$ for $\omega > \omega_R$ where ω_R is the inverse of the terminal relaxation time of the cytoskeleton network, τ_R (**Figure 3**). At high frequencies, $\omega > \omega_e$, then G' and G'' are both proportional to $\omega^{3/4}$, a power-law dependence that reflects the bending lateral fluctuations of the semiflexible filaments in the network.[70,71] The frequency ω_e is approximately equal to the inverse of the time required for lateral fluctuations to begin to touch the walls of the confining tube-like region (**Figure 3(b)**). The exponent would be $^1/_2$ instead of $^3/_4$ if the polymers constituting the cytoskeleton were flexible.[41]

In particle tracking microrheology of living cells, the size of the probing beads has to be larger than the average mesh size of the cytoskeleton, typically 50 nm for fibroblasts.[72,73] This mesh size can be measured via fluorescence recovery after photobleaching (FRAP) of fluorescently labeled dextran of various molecular weights introduced into the cell. The effective mesh size of the cytoskeleton is equal to the radius of gyration corresponding to the smallest molecular weight of dextran for which there is little or no recovery after photobleaching. Here again, without applying oscillatory deformations to the cytoplasm of the cells, the frequency-dependent viscoelastic moduli can be computed from the mean squared displacements of embedded beads. In this case, it can be shown that the viscoelastic moduli can be computed from the so-called complex modulus, $G^*(\omega)$, as:[74]

$$G^*(\omega) = \frac{2k_BT}{3\pi a i\omega F_u[<\Delta r^2(t)>]}. \qquad [7]$$

Here, $F_u[\langle \Delta r^2(t) \rangle]$ is the unilateral Fourier transform of the measured $\langle \Delta r^2(t) \rangle$. Equation [7] can be solved analytically[53] if one allows the frequency-dependent elastic modulus to be calculated algebraically using the following relationship:

$$G'(\omega) = |G^*(\omega)|\cos\left[\frac{\pi\alpha(\omega)}{2}\right] \qquad [8]$$

The amplitude $|G^*(\omega)|$ can be approximated as

$$|G^*(\omega)| \approx \frac{2k_BT}{3\pi a\langle \Delta r^2(1/\omega)\rangle\Gamma[1+\alpha(\omega)]} \qquad [9]$$

Here α is the local slope of a log–log plot of $\langle \Delta r^2(t) \rangle$ as a function of t estimated at the frequency of interest ω; Γ is the gamma function. The above expressions need to be used in the cases of cytoplasm or actin filament networks *in vitro*.

7.8.3.4 Dynamic Viscosity versus Shear Viscosity

The viscous modulus, $G''(\omega)$, or alternatively the dynamic viscosity, $\eta''(\omega) = G''(\omega)/\omega$, and the shear viscosity, η, of a material should not be confused with one another. $G''(\omega)$ represents the fraction of energy induced by the imposed deformation, which is lost by viscous dissipation as opposed to stored elasticity by the material. In a standard rheometer, $G''(\omega)$ is computed by imposing an oscillatory deformation of controlled frequency and measuring the out-of-phase component of the frequency-dependent stress induced in the material. In contrast, the shear viscosity η has units of Pa s and is measured by imposing a steady deformation of constant rate. It is the ratio of the stress induced in the material to the rate of deformation.

Here again without applying any external forces to the cytoplasm, one can compute an approximate value of its shear

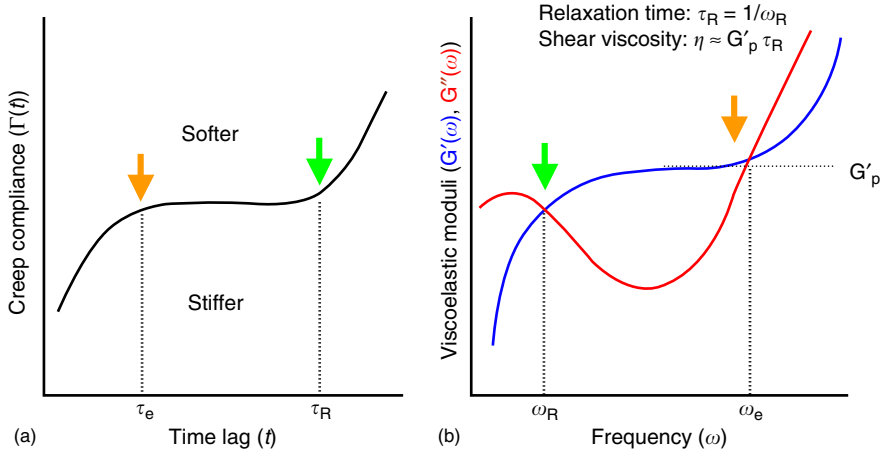

Figure 3 Creep compliance and viscoelastic moduli of the cytoplasm. (a) Typical creep compliance of the cytoplasm measured by the spontaneous displacements of beads embedded inside the cytoplasm of a living cell (see also the inset in **Figure 1(c)**). The creep compliance defines two characteristic timescales, τ_e and τ_R. (b) The frequency-dependent elastic (or storage) modulus, $G'(\omega)$, and viscous (or loss) modulus, $G''(\omega)$, of the cytoplasm can be approximately computed from the mean squared displacement of the beads or equivalently from the time-dependent creep compliance shown in (a). In general, the cytoplasm behaves as a viscoelastic liquid at low frequencies (corresponding to long timescales, $t > \tau_R$): $G''(\omega) > G'(\omega)$ for $\omega < \omega_R$. The cytoplasm behaves as a viscoelastic solid at intermediate frequencies: $G''(\omega) > G'(\omega)$ for $\omega_e > \omega > \omega_R$. Finally, the cytoplasm behaves again as a viscous liquid at high frequencies, $\omega > \omega_e$, for which $G''(\omega) \sim G'(\omega) \sim \omega^{3/4}$. Adapted with permission from Wirtz, D. Particle-tracking microrheology of living cells: principles and applications. *Annu. Rev. Biophys.* **2009**, *38*, 301–326. Copyright by Annual Reviews.

viscosity η from the frequency-dependent viscoelastic moduli, $G'(\omega)$ and $G''(\omega)$:

$$\eta \approx G'_p \tau_R \quad [10]$$

where G'_p is the plateau value of the elastic modulus $G'(\omega)$ at intermediate frequencies (between ω_e and ω_R) and τ_R, already defined above, is the inverse of the frequency ω_R at which $G'(\omega)$ and $G''(\omega)$ are equal (see definitions in **Figure 3(b)**). Typical values of shear viscosity of the cytoplasm of a wide range of cells and materials are given in **Tables 1** and **2**.

Particle tracking microrheology indicates that the rheology of the cytoplasm is not only time scale dependent, but also that the frequency-dependent viscoelastic moduli define a single crossover frequency, ω_R at low frequencies (**Figure 3(b)**). Below this frequency, the cytoplasm behaves essentially as a viscous liquid. Equivalently, in the time domain, if the cytoplasm were subjected to a step deformation, the time-dependent stress induced in the cytoplasm would adapt a plateau value at intermediate timescales, crossing over at a characteristic time τ_R ($=1/\omega_R$) to a terminal viscous relaxation at long timescales (**Figure 3(a)**).

Sometimes the MSD of beads inside a viscoelastic material can be fitted by a power law of the time lag: $\langle \Delta r^2 \rangle = Kt^\alpha$ where the exponent $\alpha \leq 1$ and K is a constant. This is also the case of foams, emulsions, and slurries. In this case, the movement of the beads are called subdiffusive or that the beads undergo anomalous diffusion. Here, the frequency-dependent elastic and viscous moduli are proportional to each other: $G'(\omega) \sim G''(\omega) \sim \omega^\alpha$. Soft glassy materials display power-law rheology described by $G'(\omega) \sim G''(\omega) \sim \omega^\alpha$. These materials do not feature a terminal relaxation time and, therefore, are not characterized by a single relaxation time, but by a broad distribution of relaxation times. Recent measurements suggest that isolated nuclei may behave as soft glassy materials.[75]

7.8.3.5 Creep Compliance from Particle Tracking Microrheology

From a rheological point of view, the cytoplasm is a viscoelastic material. As suggested above, the mathematical transformation of the measured time-dependent MSD into frequency-dependent elastic and viscous moduli, $G'(\omega)$ and $G''(\omega)$ is not trivial[53,74] (see eqns [2]–[4]). This transformation involves Fourier/Laplace integrals that presume the knowledge of the MSD over an infinite range of timescales. Therefore, large errors can be introduced in the computation of $G'(\omega)$ and $G''(\omega)$ at low and high frequencies, corresponding to the maximum time of capture (at long timescales) and the rate of image capture of the camera for the MSD (at short timescales), respectively. However, it can be shown that the mean squared displacement of a bead is proportional to the creep compliance $\Gamma(t)$ of the material in which the bead is embedded[38] (**Figures 1(c)** and **3**):

$$\Gamma(t) = \frac{3\pi a}{2k_B T}\langle \Delta r^2(t) \rangle \quad [11]$$

The creep compliance of a material is its deformability and, in classical rheological measurements, is obtained by imposing a steady mechanical stress of constant magnitude and measuring the resulting shear deformation of the material. Here again, we can compute the creep compliance from particle tracking measurements without imposing any deformations.

If we return to the examples of viscous liquid and elastic solid already described above, then simple substitution of the expressions of $\langle \Delta r^2 \rangle$, $\langle \Delta r^2 \rangle = (2k_BT/3\pi a\eta)t$ and $\langle \Delta r^2 \rangle = C$ in eqn [6] indicates that the creep compliance of a viscous liquid (no elasticity) is $\Gamma(t) = t/\eta$, while the creep compliance of a highly elastic solid (negligible viscosity) is $\Gamma(t) = (3\pi aC/2k_BT) =$ constant. Therefore, the creep compliance of a viscous liquid is inversely proportional to the shear viscosity, $\Gamma(t) \sim 1/\eta$, and the creep compliance of an elastic solid is the inverse of the material's elasticity, $\Gamma = 1/G'$ where G' is a constant.

All the rheological information about the cytoplasm or material in which the probing beads are embedded is effectively contained in the time-dependence and magnitude of creep compliance[76] (**Figure 3(a)**). To illustrate this concept, we return to the relatively simple example of a concentrated suspension of uncrosslinked actin filaments, in which beads have been embedded. This bead diameter is selected to be larger than the mesh size of the network. Hence the bead is in intimate physical contact with the filaments, which, for a finite time, form a steric "cage" that confines the bead (**Figure 1(a)**). At short timescales, the motion of the bead is dictated by the lateral fluctuations of the cage-forming filaments in contact with the bead (**Figure 1(b)**). Hence the mean squared displacement of the bead grows with time as $t^{3/4}$ (**Figure 1(c)**). A movie captured at high frame rate would show that the bead undergoes small-magnitude, random, and rapid displacements created by the lateral fluctuations of the confining filaments. At intermediate timescales, the bead does not undergo net motion anymore because the filaments surrounding the bead cannot escape from their own confining tube-like region. Finally, at long timescales, the filaments surrounding the bead can escape their tube-like regions through large-magnitude longitudinal motion (**Figure 1(b)**). Accordingly, the filamentous cage that was confining the bead disappears since its constitutive filaments have moved out of the way. A slow camera would capture the bead going from cage to cage, undergoing a random walk – albeit at a very slow pace set by the high viscosity of the actin filament solution.

7.8.4 Microrheology of Live Cells

7.8.4.1 Applications of Particle Tracking Microrheology in Cell Biology

Particle tracking microrheology – also called passive microrheology or ballistic intracellular nanorheology (BIN) – has readily demonstrated that the cytoplasm of adherent cells at rest, such as endothelial cells and fibroblasts placed on planar substrates, is typically more elastic than viscous at short timescales (i.e. these cells show a rheological behavior which is akin to that of a solid), for timescales between 0.1 and $\sim$10 s.[8] The same cells are predominantly viscous at long timescales, $>$10–20 s, for which the cytoplasm behaves like a viscous liquid.[8] Hence, for fast movements of the cells, the

cytoplasm behaves as a solid, while for slow movements of the cells, the cytoplasm behaves as a liquid.

In general, the viscoelastic properties of adherent cells are dominated by the actin filament network, and to a lesser extent by the two other major cytoskeletal filaments, microtubules and intermediate filaments. Indeed pharmacological treatment by cytochalasin D or latrunculin B, which induces the disassembly of actin filaments, dramatically increases the deformability of the cytoplasm or, equivalently, decreases the cytoplasmic stiffness or elasticity at all measured timescales.[26,77] Moreover, the degree of cytoplasmic elasticity correlates with the local concentration of F-actin (filamentous actin): the cell periphery (i.e., the lamella), which contains an actin-rich dense meshwork, is significantly stiffer than the perinuclear region, which contains significantly less actin.

Additional evidence of the critical role of actin in cell mechanics comes from microrheological studies of cells under shear. Serum-starved cells, which show little organized F-actin (filamentous actin), have both a low viscosity and a low elasticity. The same cell subjected to levels of shear stress similar to those present in blood vessels displays rapid assembly of actin filaments into organized bundled and contractile structures[10,78]. Particle tracking microrheology shows that actin filament assembly and bundling induced by extracellular flow stimulation is accompanied initially by a rapid increase in cytoplasmic stiffness, and then a rapid relaxation under continued flow stimulation.[10] This transient increase in cytoplasmic stiffness correlates with the transient activation of the Rho/ROCK-mediated pathway and the associated assembly, parallel bundling, contractility, and contractility of actin filaments by motor and F-actin bundling protein myosin II.

Endothelial and epithelial cells polarize their morphology and position their microtubule organizing center (MTOC or centrosome) towards the cell's leading edge during migration at the wound edge.[5,79] Particle tracking microrheology shows that the mechanical properties of the cytoplasm of these migrating cells become spatially polarized as well. The cytoplasm is much stiffer at the leading edge than at the trailing edge of the migrating cells.[1] Centrosome positioning at the edge of the migrating cells is abrogated in cells that are transfected with a dominant negative mutant of the small GTPase Cdc42.[80] This abrogated polarization is accompanied with the abrogated ability of these cells to polarize their mechanical properties.

Particle tracking microrheology has also shown that the elasticity of the cytoplasm is much lower than that of the nucleus in the same cell, which explains the nature of movements of nucleus within the cell. Nevertheless, similar to the cytoplasm, the nucleus is significantly more elastic than viscous,[12] albeit over a much wider range of timescales. This is an important result as cells embedded inside a 3-D matrix move though a dense crosslinked collagen-rich extracellular matrix and a rate-limiting step in 3-D migration seems to be the ability of cells to eventually squeeze their nucleus through partially digested pores.[81]

Measurements of the mean shear viscosity and the elasticity of the intranuclear region by particle tracking microrheology has determined a lower bound of the forces required for nuclear organelles such as PML bodies to undergo processive transport within the nucleus by overcoming the friction forces set by the intranuclear viscosity, $\sim$3–15 pN. Dynamic analysis of the spontaneous movements of submicron beads embedded in the nucleus also reveals the presence of transient nuclear microdomains of mean size 290 nm, which are largely absent in the cytoplasm.[12,82] The strong 'solid' character and the microorganization of the intranuclear region revealed by particle tracking analysis may help the nucleus preserve its structural coherence and organize chromosomes. We note that XX low interstitial nucleoplasmic viscosity, which controls the transport of nuclear proteins and molecules, and the much higher mesoscale viscosity, which affects the diffusion and the directed transport of nuclear organelles and reorganization of interphase chromosomes.[12]

Finally, particle tracking microrheology has shown that the unique response of human endothelial cells when inside a more physiological 3-D matrix compared to conventional substrates. The cytoplasm of matrix-embedded cells is much softer than the cytoplasm of the same cells placed on a flat substrate.[11] Moreover, exposure to vascular endothelial growth factor (VEGF), which enhances proliferation and migration of endothelial cells in the 3-D matrix, increases their elasticity and viscosity in the matrix, but not so for cells on substrates. This VEGF-induced softening response of the cytoplasm is abrogated by specific inhibition of ROCK (Rho kinase).

In typical measurements of cell mechanics (e.g., atomic force microscopy (AFM)),[83–85] it is assumed that the nucleus and the cytoplasm contribute independently to global cell stiffness. This assumption is an oversimplification that overlooks the existence of critical functional links between the nucleus and the cytoskeleton. These physical connections are established by specific linker proteins located at the nuclear envelope called the linkers of nucleus to cytoskeleton (LINC) complexes. LINC complexes form physical connections between nucleus and cytoskeleton and play as a critical role in cell mechanics as the intrinsic mechanical properties of the nucleus and the cytoskeleton themselves. Indeed, when LINC complexes are disrupted, then the elasticity of the cytoplasm is significantly reduced and the magnitude of this reduction is as important as observed when the actin cytoskeleton is completely disassembled with actin-depolymerizing drugs.[7]

Particle tracking microrheology shows that the loss of the LINC complex dramatically affects the ability of cells to resist mechanical shear forces.[20] Mutations scattered along *Lmna*, which encodes A-type lamins, have been associated with a broad range of human diseases, collectively called laminopathies.[86–91] These diseases involve either specific or combined pathologies of neurons, muscle, and bone tissue.[86,87] Cytoplasmic fragility, measured by particle tracking microrheology, correlates with the disruption of LINC complexes at the nuclear envelope in cells derived from mouse models of laminopathies.[7,20,21]

The above measurements could only be obtained by particle tracking microrheology analysis. Particle tracking microrheology can measure the mechanical properties of live cells in more physiological environments than other methods for cell mechanics. For instance, particle tracking microrheology is the only cell-mechanics method introduced so far in the literature that could probe the mechanical properties of cells embedded inside a 3-D matrix and their mechanical response to agonists and/or drug treatments,[11] monitor in real time the changes in

cytoplasmic elasticity in cells subjected to shear flows,[10] or measure *in vivo* the local viscoelastic properties of cells in a *C. elegans* developing embryo.[92] Cells in these more physiological environments than conventional flat substrates cannot be probed by other cell-mechanics methods, including AFM and magnetic/optical tweezers, because these cells are inaccessible to direct physical contact and can only be mechanically probed at a distance. Hence particle tracking microrheology presents the unique potential to be used to probe the micromechanical properties of cells in animal models, such as mice and rats. Although a direct demonstration of particle tracking microrheology in rodents is currently lacking.

Applications of particle tracking microrheology presented above were only possible thanks to the replacement of manual microinjection of beads inside cells by ballistic injection.[10,11,78] In a single ballistic injection, the number of injected cells amenable to measurements increases 1000-fold compared to conventional microinjection.[10,11] With a large sample size per condition, particle tracking microrheology results become more precise and significant. Ballistic injection of beads into the cytoplasm combined with particle tracking (ballistic injection nanorheology or BIN) provides consistent values of cellular viscoelastic properties.

7.8.4.2 Interstitial Viscosity versus Mesoscale Viscoelasticity of the Cytoplasm

The viscosity of the intracellular space depends critically on the length scale being probed. At small length scales, the viscosity of the cytoplasm is essentially that of water (more precisely, 1.2–1.4 times the viscosity of water[93]) or approximately 0.01 Poise.[94,95] It can be measured by monitoring the diffusion of GFP or small fluorescently labeled DNA fragments in the cell. This interstitial viscosity is a key parameter that controls the transport of small globular proteins and it varies slightly for various cell conditions.

At length scales larger than the effective mesh size of the cytoskeleton meshwork, the apparent viscosity is much higher, typically >10 Poise or 1000 times the viscosity of water. This 'effective' mesh size can be measured by probing the diffusion of fluorescently labeled dextran or DNA inside the cell. The diffusion of dextran polymers of radius of gyration <50 nm diffuse within the cytoplasm (of fibroblasts) is largely unhindered, while polymers >50 nm become 'immobilized'.[73,94,95] At length scales larger than the effective mesh size of the cytoplasm, the viscoelastic moduli and creep compliance computed from particle tracking measurements should be independent of the size of the probe beads used in the experiments. This is readily seen from the expression in eqn [1] in the limit case of a viscous liquid: the creep compliance depends linearly on both bead size and MSD, which itself depends inversely on bead size.

The above discussion about how viscoelastic parameters of the cytoplasm can be obtained from particle tracking measurements assumes that the probing beads are larger than the effective mesh size of the cytoplasm or the network being probed (**Figure 4**). We call this viscosity, mesoscale viscosity, as it describes the rheological properties at length scales intermediate between small globular proteins in the interstitial space and the whole cell. The mesoscale viscosity controls the rate of movements of mitochondria,[96] nucleus,[5] and phagosomes,[97] as well as viruses, bacteria, engineered drug delivery microcarriers,[97] because these entities are larger than the effective mesh size of the cytoskeleton. The mesoscale viscosity of the cytoplasm also controls the rates of cell spreading and migration.[98]

7.8.4.3 Active versus Passive Microrheology of Cells

Direct injection of the beads into the cytoplasm,[8] as opposed to passive engulfment of the beads inside the cytoplasm, circumvents the endocytic pathway and, therefore, the engulfment of the beads in vesicles tethered to cytoskeleton filaments by motor proteins.[97] These vesicles move towards the nucleus, therefore the probe beads would undergo directed motion. While interesting in its own right, such directed displacements would prevent the computation of the viscoelastic parameters of the cytoplasm from mean squared displacements.

Nevertheless, even in the absence of directed motion, acto-myosin contractility could affect the movements of beads. Recent work with reconstituted actin filament networks containing myosin II has shown that, in this *in vitro* system, the movements of beads can be affected 10 fold, and even greater at long timescales by the activity of motor proteins.[99] Even without producing a net movement of the filaments, motor proteins enhance the random movements of the beads, which is akin to an effective increase of the temperature of the system more than 10 fold.[99] These enhanced movements allow for faster relaxation of mechanical stresses. This result obtained with purified proteins suggests that particle tracking measurements of the mechanical properties of the cytoplasm would significantly underestimate the values of the viscoelastic properties of the cytoplasm in live cells.

However, recent results suggest that reducing or eliminating acto-myosin contractility in a live cell using either blebbistatin, which blocks the myosin heads in a complex with low actin affinity,[100] or ML-7, which specifically inhibits MLCK (myosin light chain kinase) which normally phosphorylates myosin II, has no significant effect on the magnitude of the displacements of the beads compared to control cells.[101] This absence of effect may be due in part to the fact that myosin II molecules are mostly localized to the contractile actin stress fibers localized to the ventral side of the cell and the leading edge, and are not present in large quantities in the body of the cell,[27] where beads used for particle tracking microrheology are lodged. Therefore, it is clear that a direct extrapolation of results obtained *in vitro* with purified proteins, while often instructive of the more complex behavior of cytoskeleton in cells,[102] can be misleading.

The movements of the cell itself can add an additional contribution to the overall movements of the probing beads. The speed of adherent cells[103] is typically much lower than the speed of the probing beads embedded in the cytoplasm. Therefore, the movements of the cell will be felt by the beads embedded in the cytoplasm only when they are monitored for a long time. The contribution of cell movements to the overall movements of the beads can readily be detected by the

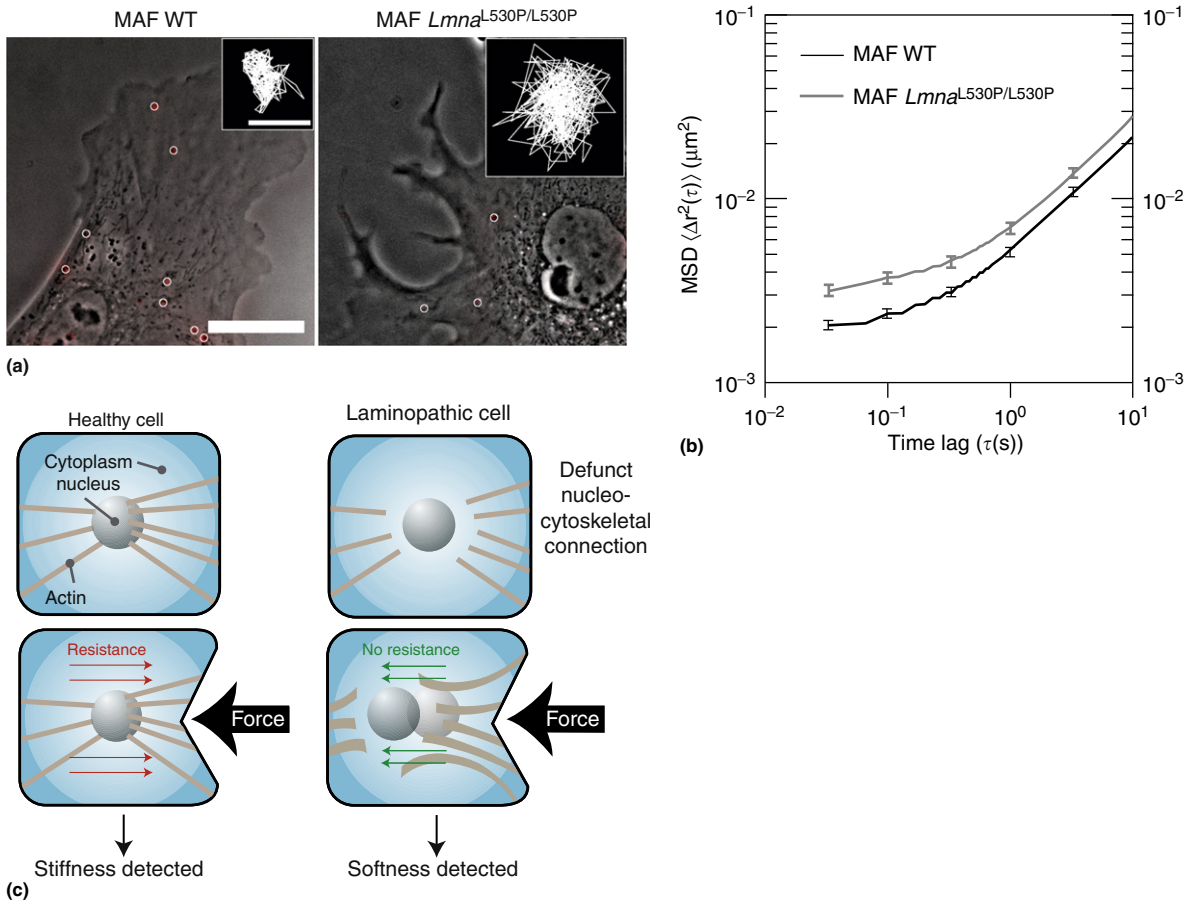

Figure 4 Intracellular microrheology of laminopathic fibroblasts. (a) Fluorescent 100 nm diameter polystyrene beads are ballistically injected in wildtype (left panel) and *Lmna*$^{L530P/L530P}$ (right panel) adult fibroblasts (MAFs), derived from a mouse model of progeria. Fluorescent micrographs of beads (outlined in white circles) are superimposed on phase-contrast micrographs of cells. Representative trajectories of nanoparticles are shown at the top right (inset) of each micrograph. Micrograph scale bar, 20 μm; inset scale bar, 0.1 μm. (b) Ensemble-averaged mean squared displacements of the beads embedded in the cytoplasm of wild type (bottom black curve) and *Lmna*$^{L530P/L530P}$ (top gray curve) MAFs are shown. (c) Model for the intracellular mechanics of healthy and laminopathic cells. Healthy cells in which the nucleo-cytoskeletal connections are intact can resist forces of large magnitude, while laminopathic cells cannot resist such forces due to defunct nucleo-cytoskeletal connections. Taken from Hale, C. M.; Shrestha, A. L.; Khatau, S. B.; Stewart-Hutchinson, P. J.; Hernandez, L.; Stewart, C. L.; Hodzic, D.; Wirtz, D. Dysfunctional connections between the nucleus and the actin and microtubule networks in laminopathic models. *Biophys. J.* **2008**, 95(11), 5462–5475.

curvature of the mean square displacements of the embedded beads. To illustrate this effect, we consider the simple case of a viscous liquid. If an overall movement is added to the thermally-driven random motion of the bead, then the MSD can be rewritten as:[52]

$$\langle \Delta r^2 \rangle = 4Dt + \mathrm{v}^2 t^2 \qquad [12]$$

where v is the overall speed of the suspending liquid. The first term in this expression corresponds to the random thermally-driven motion of the bead, while the second term corresponds to the motion of the bead imposed by the overall movement of the liquid. At short times scales, the second term is negligible and we recover $\langle \Delta r^2 \rangle \approx 4Dt$, that is, bead movements are dominated by viscous diffusion. At long timescales, the second term dominates, $\langle \Delta r^2 \rangle \approx \mathrm{v}^2 t^2$, corresponding to a quadratic dependence on time, which is readily observed at long times in the MSD profile. The timescale at which the crossover between these two regimes occurs (when $4Dt = \mathrm{v}^2 t^2$) is $t = 4D/\mathrm{v}^2$. For instance, for a 100 nm diameter bead in a 20 Poise viscous liquid, $D \approx 0.0022\ \mu\mathrm{m}^2\ \mathrm{s}^{-1}$, moving at a constant speed of $5\ \mu\mathrm{m\ h}^{-1}$ (a typical speed for a cultured adherent cell), the crossover time is equal to $t = 4D/\mathrm{v}^2 = 1.3$ s, which is readily detected when tracking a bead for 10 s.

7.8.4.4 Advantages of Particle Tracking Microrheology

Particle tracking microrheology can measure directly the mechanical properties of the cytoplasm that it is embedded in.[12] In contrast, most current single-cell mechanics methods rely on a direct contact between the cell surface and a physical probe. For example, an AFM probes the mechanical properties of cells using soft cantilevers,[104] while magnetocytometry[105,106] measures cell mechanics by subjecting large beads coated with ECM molecules bound to cell receptors to rotational movements. These methods cannot directly

distinguish the contribution of the plasma membrane from the combined response of the nucleus and the cytoplasm without making drastic assumptions. If two elastic elements of different stiffness are connected to one another (here the nucleus and the cytoskeleton), their total response is dominated by the stiffer element. Therefore, methods such as AFM, magnetocytometry or micropipette suction measure the combined response of the nucleus and cytoplasm, even when the probe is positioned far away from the nucleus. In contrast, particle tracking microrheology, which relies on the smallest energy possible – the thermal energy – provides for highly localized measurement inside the cytoplasm.

Unlike most other approaches in cell mechanics, particle tracking microrheology measures frequency-rate dependent viscoelastic moduli, $G'(\omega)$ and $G''(\omega)$. As discussed in detail above, this is particularly crucial for the cytoskeleton. The frequency-dependent mechanical response of the cytoplasm of a live cell can be measured in about 10 s by particle tracking microrheology, a timescale relevant to cell motility. In contrast, AFM measurements may take up to 1h for high-resolution mechanical measurements.[85] Such time-consuming measurements cannot capture fast subcellular dynamics and are unsuitable for highly motile cells, such as cancer cells.

Particle tracking microrheology requires short times of data collection, typically 10–20 s in order to measure frequency-dependent viscoelastic moduli over two decades in frequency (or timescales). This is not the case for other particle tracking methods where the correlated motion between two particles is used instead of the motion of individual particles as a probe of local cytoplasmic rheology.[66] These methods are not suitable for mechanical measurements of live cells since they incorrectly assume that the intracellular milieu is homogeneous. Furthermore, to obtain statistically significant data, measurements last 30–60 min, timescales for which migrating cells cannot be assumed to be stationary.

By tracking multiple beads in the field of view simultaneously, microrheology can measure the micromechanical responses to stimuli in various parts of the cell simultaneously. This is particularly important since it is now clear that the viscoelastic properties can vary by more than two orders of magnitude within the same cell.[8,12,107] Moreover, by using video-based multiple particle tracking instead of laser-deflection particle tracking,[26,53] 10–100's of beads embedded in the cytoplasm can be tracked simultaneously.

Particle tracking microrheology measurements of the cytoplasm of live cells are typically conducted using carboxylated polystyrene beads or PEG-coated beads. The rheology of reconstituted actin filament networks or DNA solutions measured by particle tracking microrheology and using these beads is quantitatively similar to that measured by a standard rheometer.[38,61] This agreement suggests that the presence of the beads in polymer networks or in the cell does not affect their mechanical properties. Moreover, carboxylated polystyrene beads or PEG-coated beads, but not amino-modified beads, yield the same frequency-dependent viscoelastic moduli for the cytoplasm of fibroblasts.[8] The proximity of the plasma membrane to some of the embedded beads near will not significantly affect the movements of the beads because hydrodynamic interactions caused by the movements of the beads and reflecting on the membrane are screened by the cytoskeleton mesh within a distance equals to the mesh size, ~50 nm.[26,41] Subcellular organelles can also be used as probing particles.[26,67,71] However, since organelle-bead interactions are not well defined, only the frequency dependence of the viscoelastic moduli is meaningful, at least at high frequency, not the magnitude of the computed moduli.

Microrheological measurements are absolute and compare favorably with traditional rheometric measurements of standard fluids of known viscosity and elasticity.[38,53,108,109] This is not the case of some single-cell approaches that rely on a direct physical contact between the cell surface and the probe (such as a cantilever or a macroscopic bead, etc.). For instance, the apparent viscoelastic moduli measured by magnetocytometry and AFM depend greatly on the type of ligands coated on the magnetic beads or the AFM cantilever. Extracellular matrix ligands – including fibronectin or RGD peptide – coated on magnetic beads and AFM cantilevers lead to vastly different values of (apparent) cell stiffness. Therefore the measurements of viscoelastic properties of standard materials using these methods cannot be directly compared to those obtained using a rheometer. Furthermore, particle tracking microrheology measures both elasticity and viscosity, while many other approaches cannot directly distinguish the elastic from the viscous response of a cell.

Importantly, values of shear viscosity and elastic moduli of the cytoplasm in live cells measured by particle tracking microrheology (**Table 1**) are similar to those measured in 'reconstituted' actin filament networks in the presence of crosslinking/bundling proteins (**Table 2**). The elasticity of cells, such as mouse embryonic fibroblasts or human umbilical vein endothelial cells, which are commonly used as models of cell biology, and of reconstituted actin filament networks are both in the order of tens of Pascal (100's of dyne cm^{-2}). This is in contrast to values of cell elasticity obtained using an AFM, which is of the order of hundreds and even thousands of Pascal.[85] To our knowledge, no actin filament network reconstituted *in vitro* containing a physiological concentration of actin polymerized in the presence of crosslinking and bundling proteins, as well as motor proteins, and under mechanical tension (which can further increase the network elasticity) has been shown to reach kPa levels of elasticity.[45] The discrepancy between values of cell elasticity measured by AFM and those obtained with actin filament networks by conventional rheometry or particle tracking microrheology remains unexplained.

Acknowledgments

The author thanks members of the Wirtz group who developed, tested, and used the method of particle tracking microrheology presented in this chapter. Work in the author's laboratory is supported by the National Institutes of Health grants GM084204 and CA143868.

References

[1] Kole, T. P.; Tseng, Y.; Jiang, I.; Katz, J. L.; Wirtz, D. Intracellular mechanics of migrating fibroblasts. *Mol. Biol. Cell.* **2005**, *16*, 328–338.

[2] Pollard, T. D.; Borisy, G. G. Cellular motility driven by assembly and disassembly of actin filaments. *Cell* **2003**, *112*, 453–465.

[3] Lammerding, J.; Schulze, P. C.; Takahashi, T.; Kozlov, S.; Sullivan, T.; Kamm, R. D.; Stewart, C. L.; Lee, R. T. Lamin A/C deficiency causes defective nuclear mechanics and mechanotransduction. *J. Clin. Invest.* **2004**, *113*, 370–378.

[4] Lammerding, J.; Lee, R. T. The nuclear membrane and mechanotransduction: impaired nuclear mechanics and mechanotransduction in lamin A/C deficient cells. *Novartis Found. Symp.* **2005**, *264*, 264–273, discussion 273–278.

[5] Lee, J. S.; Chang, M. I.; Tseng, Y.; Wirtz, D. Cdc42 mediates nucleus movement and MTOC polarization in Swiss 3T3 fibroblasts under mechanical shear stress. *Mol. Biol. Cell.* **2005**, *16*, 871–880.

[6] Minin, A. A.; Kulik, A. V.; Gyoeva, F. K.; Li, Y.; Goshima, G.; Gelfand, V. I. Regulation of mitochondria distribution by RhoA and formins. *J. Cell Sci.* **2006**, *119*, 659–670.

[7] Lee, J. S.; Hale, C. M.; Panorchan, P.; Khatau, S. B.; George, J. P.; Tseng, Y.; Stewart, C. L.; Hodzic, D.; Wirtz, D. Nuclear lamin A/C deficiency induces defects in cell mechanics, polarization, and migration. *Biophys. J.* **2007**, *93*, 2542–2552.

[8] Tseng, Y.; Kole, T. P.; Wirtz, D. Micromechanical mapping of live cells by multiple-particle-tracking microrheology. *Biophys. J.* **2002**, *83*, 3162–3176.

[9] Wirtz, D. Particle-tracking microrheology of living cells: principles and applications. *Annu. Rev. Biophys.* **2009**, *38*, 301–326.

[10] Lee, J. S.; Panorchan, P.; Hale, C. M.; Khatau, S. B.; Kole, T. P.; Tseng, Y.; Wirtz, D. Ballistic intracellular nanorheology reveals ROCK-hard cytoplasmic stiffening response to fluid flow. *J. Cell Sci.* **2006**, *119*, 1760–1768.

[11] Panorchan, P.; Lee, J. S.; Kole, T. P.; Tseng, Y.; Wirtz, D. Microrheology and ROCK signaling of human endothelial cells embedded in a 3-D matrix. *Biophys. J.* **2006**, *91*, 3499–3507.

[12] Tseng, Y.; Lee, J. S.; Kole, T. P.; Jiang, I.; Wirtz, D. Micro-organization and visco-elasticity of the interphase nucleus revealed by particle nanotracking. *J. Cell Sci.* **2004**, *117*, 2159–2167.

[13] Rogers, S. S.; Waigh, T. A.; Lu, J. R. Intracellular microrheology of motile Amoeba proteus. *Biophys. J.* **2008**, *94*, 3313–3322.

[14] Jonas, M.; Huang, H.; Kamm, R. D.; So, P. T. Fast fluorescence laser tracking microrheometry, II: quantitative studies of cytoskeletal mechanotransduction. *Biophys. J.* **2008**, *95*, 895–909.

[15] Crocker, J. C.; Hoffman, B. D. Multiple-particle tracking and two-point microrheology in cells. *Methods Cell. Biol.* **2007**, *83*, 141–178.

[16] Lau, A. W.; Hoffman, B. D.; Davies, A.; Crocker, J. C.; Lubensky, T. C. Microrheology, stress fluctuations, and active behavior of living cells. *Phys. Rev. Lett.* **2003**, *91*, 198101.

[17] Pai, A.; Sundd, P.; Tees, D. F. In situ Microrheological Determination of Neutrophil Stiffening Following Adhesion in a Model Capillary. *Ann. Biomed. Eng.* **2008**, *36*, 596–603.

[18] Massiera, G.; Van Citters, K. M.; Biancaniello, P. L.; Crocker, J. C. Mechanics of single cells: rheology, time dependence, and fluctuations. *Biophys. J.* **2007**, *93*, 3703–3713.

[19] Sivaramakrishnan, S.; DeGiulio, J. V.; Lorand, L.; Goldman, R. D.; Ridge, K. M. Micromechanical properties of keratin intermediate filament networks. *Proc. Natl. Acad. Sci. USA* **2008**, *105*, 889–894.

[20] Stewart-Hutchinson, P. J.; Hale, C. M.; Wirtz, D.; Hodzic, D. Structural requirements for the assembly of LINC complexes and their function in cellular mechanical stiffness. *Exp. Cell Res.* **2008**, *314*, 1892–1905.

[21] Hale, C. M.; Shrestha, A. L.; Khatau, S. B.; Stewart-Hutchinson, P. J.; Hernandez, L.; Stewart, C. L.; Hodzic, D.; Wirtz, D. Dysfunctional connections between the nucleus and the actin and microtubule networks in laminopathic models. *Biophys. J.* **2008**, *95*(11), 5462–5475.

[22] Kole, T. P.; Tseng, Y.; Huang, L.; Katz, J. L.; Wirtz, D. Rho kinase regulates the intracellular micromechanical response of adherent cells to rho activation. *Mol. Biol. Cell* **2004**, *15*, 3475–3484.

[23] Ferry, J. D. *Viscoelastic Properties of Polymers*; John Wiley and Sons: New York, 1980.

[24] Xu, J.; Tseng, Y.; Wirtz, D. Strain-hardening of actin filament networks – Regulation by the dynamic crosslinking protein α-actinin. *J. Biol. Chem.* **2000**, *275*, 35886–35892.

[25] Storm, C.; Pastore, J. J.; MacKintosh, F. C.; Lubensky, T. C.; Janmey, P. A. Nonlinear elasticity in biological gels. *Nature* **2005**, *435*, 191–194.

[26] Yamada, S.; Wirtz, D.; Kuo, S. C. Mechanics of living cells measured by laser tracking microrheology. *Biophys. J.* **2000**, *78*, 1736–1747.

[27] Verkhovsky, A. B.; Svitkina, T. M.; Borisy, G. G. Myosin II filament assemblies in the active lamella of fibroblasts: their morphogenesis and role in the formation of actin filament bundles. *J. Cell Biol.* **1995**, *131*, 989–1002.

[28] Svitkina, T. M.; Verkhovsky, A. B.; McQuade, K. M.; Borisy, G. G. Analysis of the actin-myosin II system in fish epidermanl keratocytes: mechanism of cell body translocation. *J. Cell Biol.* **1997**, *139*, 397–414.

[29] Gittes, F.; Mickey, B.; Nettleton, J.; Howard, J. Flexural rigidity of microtubules and actin filaments measured from thermal fluctuations in shape. *J. Cell Biol.* **1993**, *120*, 923–934.

[30] Janmey, P. A. Mechanical properties of cytoskeletal polymers. *Curr. Op. Cell Biol.* **1991**, *2*, 4–11.

[31] Kas, J.; Strey, H.; Tang, J. X.; Fanger, D.; Sackmann, E.; Janmey, P. F-actin, a model polymer for semiflexible chains in dilute, semidilute, and liquid crystalline solutions. *Biophys. J.* **1996**, *70*, 609–625.

[32] Bausch, A.; Kroy, K. A bottom-up approach to cell mechanics. *Nature Phy.* **2006**, 231–238.

[33] de Gennes, P.-G. *Scaling Concepts in Polymer Physics*; Cornell University Press: Ithaca, 1991.

[34] de Gennes, P.-G.; Leger, L. Dynamics of entangled polymer chains. *Ann. Rev. Phys. Chem.* **1982**, *33*, 49–61.

[35] Kas, J.; Strey, H.; Sackmann, E. Direct imaging of reptation for semiflexible actin filaments. *Nature* **1994**, *368*, 226–229.

[36] Morse, D. C. Viscoelasticity of concentrated isotropic solutions of semiflexible polymers. 1. Model and stress tensor. *Macromolecules* **1998**, *31*, 7030–7043.

[37] Hinner, B.; Tempel, M.; Sackmann, E.; Kroy, K.; Frey, E. Entanglement, elasticity, and viscous relaxation of actin solutions. *Phys. Rev. Lett.* **1998**, *81*, 2614–2617.

[38] Xu, J.; Viasnoff, V.; Wirtz, D. Compliance of actin filament networks measured by particle-tracking microrheology and diffusing wave spectroscopy. *Rheologica. Acta.* **1998**, *37*, 387–398.

[39] Palmer, A.; Xu, J.; Kuo, S. C.; Wirtz, D. Diffusing wave spectroscopy microrheology of actin filament networks. *Biophys. J.* **1999**, *76*, 1063–1071.

[40] Janmey, P. A.; Hvidt, S.; Lamb, J.; Stossel, T. P. Resemblance of actin-binding protein/actin gels to covalently networks. *Nature* **1990**, *345*, 89–92.

[41] Doi, M.; Edwards, S. F. *The Theory of Polymer Dynamics*; Clarendon Press: Oxford, 1989.

[42] Wachsstock, D.; Schwarz, W. H.; Pollard, T. D. Crosslinker dynamics determine the mechanical properties of actin gels. *Biophys. J.* **1994**, *66*, 801–809.

[43] Wolf, K.; Mazo, I.; Leung, H.; Engelke, K.; von Andrian, U. H.; Deryugina, E. I.; Strongin, A. Y.; Brocker, E. B.; Friedl, P. Compensation mechanism in tumor cell migration: mesenchymal-amoeboid transition after blocking of pericellular proteolysis. *J. Cell Biol.* **2003**, *160*, 267–277.

[44] Wachsstock, D.; Schwarz, W. H.; Pollard, T. D. Affinity of a-actinin for actin determines the structure and mechanical properties of actin filament gels. *Biophys. J.* **1993**, *65*, 205–214.

[45] Tseng, Y.; An, K. M.; Esue, O.; Wirtz, D. The bimodal role of filamin in controlling the architecture and mechanics of F-actin networks. *J. Biol. Chem.* **2004**, *279*, 1819–1826.

[46] Flanagan, L. A.; Chou, J.; Falet, H.; Neujahr, R.; Hartwig, J. H.; Stossel, TP. Filamin A, the Arp2/3 complex, and the morphology and function of cortical actin filaments in human melanoma cells. *J. Cell Biol.* **2001**, *155*, 511–517.

[47] Xu, J.; Wirtz, D.; Pollard, T. D. Dynamic cross-linking by alpha-actinin determines the mechanical properties of actin filament networks. *J. Biol. Chem.* **1998**, *273*, 9570–9576.

[48] Khatau, S. B.; Hale, C. M.; Stewart-Hutchinson, P. J.; Patel, M. S.; Stewart, C. L.; Searson, P. C.; Hodzic, D.; Wirtz, D. A perinuclear actin cap regulates nuclear shape. *Proc. Natl. Acad. Sci. USA* **2009**, *106*, 19017–19022.

[49] Tseng, Y.; Kole, T. P.; Lee, J. S.; Fedorov, E.; Almo, S. C.; Schafer, B. W.; Wirtz, D. How actin crosslinking and bundling proteins cooperate to generate an enhanced cell mechanical response. *Biochem. Biophys. Res. Commun.* **2005**, *334*, 183–192.

[50] Tseng, Y.; Schafer, B. W.; Almo, S. C.; Wirtz, D. Functional synergy of actin filament cross-linking proteins. *J. Biol. Chem.* **2002**, *277*, 25609–25616.

[51] Berg, H. C. *Random Walks in Biology*; Princeton University Press: Princeton, NJ, 1993.

[52] Qian, H.; Sheetz, M. P.; Elson, E. L. Single particle tracking. Analysis of diffusion and flow in two-dimensional systems. *Biophys. J.* **1991**, *60*, 910–921.

[53] Mason, T. G.; Ganesan, K.; van Zanten, J. V.; Wirtz, D.; Kuo, S. C. Particle-tracking microrheology of complex fluids. *Phys. Rev. Lett.* **1997**, *79*, 3282–3285.

[54] Bloom, R. J.; George, J. P.; Celedon, A.; Sun, S. X.; Wirtz, D. Mapping local matrix remodeling induced by a migrating tumor cell using three-dimensional multiple-particle tracking. *Biophys. J.* **2008**, *95*, 4077–4088.

[55] Desai, K. V.; Bishop, T. G.; Vicci, L.; O'Brien, E. T.; Taylor, R. M.; Superfine, R. Agnostic particle tracking for three-dimensional motion of cellular granules and membrane-tethered bead dynamics. *Biophys. J.* **2008**, *94*, 2374–2384.

[56] Hasnain, I. A.; Donald, A. M. Microrheological characterization of anisotropic materials. *Phys. Rev. E Stat. Nonlin. Soft Matter Phys.* **2006**, *73*, 031901.

[57] Tseng, Y.; An, K. M.; Wirtz, D. Microheterogeneity controls the rate of gelation of actin filament networks. *J. Biol. Chem.* **2002**, *277*, 18143–18150.

[58] Tseng, Y.; Wirtz, D. Mechanics and multiple-particle tracking microheterogeneity of alpha-actinin-cross-linked actin filament networks. *Biophys. J.* **2001**, *81*, 1643–1656.

[59] Rudnick, J.; Gaspari, G. The shapes of random walks. *Science* **1987**, *237*, 384–389.

[60] Haber, C.; Ruiz, S. A.; Wirtz, D. Shape anisotropy of a single random-walk polymer. *Proc. Natl. Acad. Sci. USA* **2000**, *97*, 10792–10795.

[61] Palmer, A.; Xu, J.; Wirtz, D. High-frequency rheology of crosslinked actin networks measured by diffusing wave spectroscopy. *Rheologica Acta* **1998**, *37*, 97–108.

[62] Smith, S. B.; Finzi, L.; Bustamante, C. Direct mechanical measurements of the elasticity of single DNA molecules by using magnetic beads. *Science* **1992**, *258*, 1122–1126.

[63] Girard, K. D.; Kuo, S. C.; Robinson, D. N. Dictyostelium myosin II mechanochemistry promotes active behavior of the cortex on long timescales. *Proc. Natl. Acad. Sci. USA* **2006**, *103*, 2103–2108.

[64] Girard, K. D.; Chaney, C.; Delannoy, M.; Kuo, S. C.; Robinson, D. N. Dynacortin contributes to cortical viscoelasticity and helps define the shape changes of cytokinesis. *Embo. J.* **2004**, *23*, 1536–1546.

[65] Crocker, J. C.; Grier, D. G. Methods of digital video microscopy for colloidal studies. *J. Colloid Interface Sci.* **1996**, *179*, 298–310.

[66] Crocker, J. C.; Valentine, M. T.; Weeks, E. R.; Gisler, T.; Kaplan, P. D.; Yodh, A. G.; Weitz, D. A. Two-point microrheology of inhomogeneous soft materials. *Phys. Rev. Lett.* **2000**, *85*, 888–891.

[67] Rogers, S. S.; Waigh, T. A.; Zhao, X.; Lu, J. R. Precise particle tracking against a complicated background: polynomial fitting with Gaussian weight. *Phys. Biol.* **2007**, *4*, 220–227.

[68] Savin, T.; Doyle, P. S. Role of a finite exposure time on measuring an elastic modulus using microrheology. *Phys. Rev. E Stat. Nonlin. Soft Matter Phys.* **2005**, *71*, 041106.

[69] Savin, T.; Doyle, P. S. Static and dynamic errors in particle tracking microrheology. *Biophys. J.* **2005**, *88*, 623–638.

[70] Schnurr, B.; Gittes, F.; MacKintosh, F. C.; Schmidt, C. F. Determining microscopic viscoelasticity in flexible and semiflexible polymer networks from thermal fluctuations. *Macromolecules* **1997**, *30*, 7781–7792.

[71] Hoffman, B. D.; Massiera, G.; Van Citters, K. M.; Crocker, J. C. The consensus mechanics of cultured mammalian cells. *Proc. Natl. Acad. Sci. USA* **2006**, *103*, 10259–10264.

[72] Luby-Phelps, K.; Castle, P. E.; Taylor, D. L.; Lanni, F. Hindered diffusion of inert tracer particles in the cytoplasm of mouse 3T3 cells. *Proc. Natl. Acad. Sci. USA* **1987**, *84*, 4910–4913.

[73] Luby-Phelps, K.; Taylor, D. L.; Lanni, F. Probing the structure of cytoplasm. *J. Cell Biol.* **1986**, *102*, 2015–2022.

[74] Mason, T. G.; Weitz, D. Optical measurements of frequency-dependent linear viscoelastic moduli of complex fluids. *Phys. Rev. Lett.* **1995**, *74*, 1254–1256.

[75] Dahl, K. N.; Engler, A. J.; Pajerowski, J. D.; Discher, D. E. Power-law rheology of isolated nuclei with deformation mapping of nuclear substructures. *Biophys. J.* **2005**, *89*, 2855–2864.

[76] Stamenovic, D.; Rosenblatt, N.; Montoya-Zavala, M.; Matthews, B. D.; Hu, S.; Suki, B.; Wang, N.; Ingber, DE. Rheological behavior of living cells is timescale-dependent. *Biophys. J.* **2007**, *93*, L39–41.

[77] Van Citters, K. M.; Hoffman, B. D.; Massiera, G.; Crocker, J. C. The role of F-actin and myosin in epithelial cell rheology. *Biophys. J.* **2006**, *91*, 3946–3956.

[78] Panorchan, P.; Lee, J. S.; Daniels, B. R.; Kole, T. P.; Tseng, Y.; Wirtz, D. Probing cellular mechanical responses to stimuli using ballistic intracellular nanorheology. *Methods Cell Biol.* **2007**, *83*, 115–140.

[79] Gomes, E. R.; Jani, S.; Gundersen, G. G. Nuclear movement regulated by Cdc42, MRCK, myosin, and actin flow establishes MTOC polarization in migrating cells. *Cell* **2005**, *121*, 451–463.

[80] Tapon, N.; Hall, A. Rho, Rac and Cdc42 GTPases regulate the organization of the actin cytoskeleton. *Curr. Op. Cell Biol.* **1997**, *9*, 86–92.

[81] Lammermann, T.; Bader, B. L.; Monkley, S. J.; Worbs, T.; Wedlich-Soldner, R.; Hirsch, K.; Keller, M.; Forster, R.; Critchley, D. R.; Fassler, R.; Sixt, M. Rapid leukocyte migration by integrin-independent flowing and squeezing. *Nature* **2008**, *453*, 51–55.

[82] Gorisch, S. M.; Wachsmuth, M.; Ittrich, C.; Bacher, C. P.; Rippe, K.; Lichter, P. Nuclear body movement is determined by chromatin accessibility and dynamics. *Proc. Natl. Acad. Sci. USA* **2004**, *101*, 13221–13226.

[83] Radmacher, M.; Cleveland, J. P.; Fritz, M.; Hansma, H. G.; Hansma, P. K. Mapping interaction forces with the atomic force microscope. *Biophys. J.* **1994**, *66*, 2159–2165.

[84] Radmacher, M.; Fritz, M.; Kacher, C. M.; Cleveland, J. P.; Hansma, P. K. Measuring the viscoelastic properties of human platelets with the atomic force microscope. *Biophys. J.* **1996**, *70*, 556–567.

[85] Radmacher, M. Studying the mechanics of cellular processes by atomic force microscopy. *Methods Cell Biol.* **2007**, *83*, 347–372.

[86] Ben Yaou, R.; Muchir, A.; Arimura, T.; Massart, C.; Demay, L; Richard, P.; Bonne, G. Genetics of laminopathies. *Novartis Found Symp.* **2005**, *264*, 81–90, discussion 90–97, 227–230.

[87] Jacob, K. N.; Garg, A. Laminopathies: multisystem dystrophy syndromes. *Mol. Genet. Metab.* **2006**, *87*, 289–302.

[88] Broers, J. L.; Hutchison, C. J.; Ramaekers, F. C. *Laminopathies. J. Pathol.* **2004**, *204*, 478–488.

[89] Gruenbaum, Y.; Margalit, A.; Goldman, R. D.; Shumaker, D. K.; Wilson, K. L. The nuclear lamina comes of age. *Nat. Rev. Mol. Cell Biol.* **2005**, *6*, 21–31.

[90] Capell, B. C.; Collins, F. S. Human laminopathies: nuclei gone genetically awry. *Nat. Rev. Genet.* **2006**, *7*, 940–952.

[91] Mounkes, L.; Kozlov, S.; Burke, B.; Stewart, C. L. The laminopathies: nuclear structure meets disease. *Curr. Opin. Genet. Dev.* **2003**, *13*, 223–230.

[92] Daniels, B. R.; Masi, B. C.; Wirtz, D. Probing single-cell micromechanics in vivo: the microrheology of C. elegans developing embryos. *Biophys. J.* **2006**, *90*, 4712–4719.

[93] Fushimi, K.; Verkman, A. S. Low viscosity in the aqueous domain of cell cytoplasm measured by picosecond polarization microfluorimetry. *J. Cell Biol.* **1991**, *112*, 719–725.

[94] Lukacs, G. L.; Haggie, P.; Seksek, O.; Lechardeur, D.; Freedman, N.; Verkman, A. S. Size-dependent DNA mobility in cytoplasm and nucleus. *J. Biol. Chem.* **2000**, *275*, 1625–1629.

[95] Seksek, O.; Biwersi, J.; Verkman, A. S. Translational diffusion of macromolecule-sized solutes in cytoplasm and nucleus. *J. Cell Biol.* **1997**, *138*, 131–142.

[96] Lacayo, C. I.; Theriot, J. A. Listeria monocytogenes actin-based motility varies depending on subcellular location: a kinematic probe for cytoarchitecture. *Mol. Biol. Cell* **2004**, *15*, 2164–2175.

[97] Suh, J.; Wirtz, D.; Hanes, J. Efficient active transport of gene nanocarriers to the cell nucleus. *Proc. Natl. Acad. Sci. USA* **2003**, *100*, 3878–3882.

[98] Gupton, S. L.; Anderson, K. L.; Kole, T. P.; Fischer, R. S.; Ponti, A.; Hitchcock-DeGregori, S. E.; Danuser, G.; Fowler, V. M.; Wirtz, D.; Hanein, D.; Waterman-Storer, C. M. Cell migration without a lamellipodium: translation of actin dynamics into cell movement mediated by tropomyosin. *J. Cell Biol.* **2005**, *168*, 619–631.

[99] Mizuno, D.; Tardin, C.; Schmidt, C. F.; Mackintosh, F. C. Nonequilibrium mechanics of active cytoskeletal networks. *Science* **2007**, *315*, 370–373.

[100] Kovacs, M.; Toth, J.; Hetenyi, C.; Malnasi-Csizmadia, A.; Sellers, J. R. Mechanism of blebbistatin inhibition of myosin II. *J. Biol. Chem.* **2004**, *279*, 35557–35563.

[101] Hale, C. M.; Sun, S. X.; Wirtz, D. Resolving the role of actoymyosin contractility in cell microrheology. *PLoS One* **2009**, *4*, e7054.

[102] Pollard, T. D. The cytoskeleton, cellular motility and the reductionist agenda. *Nature* **2003**, *422*, 741–745.

[103] Bray, D. *Cell Movements: From Molecules to Motility*; Garland Publishing: New York, 2001.

[104] Hoh, J. H.; Schoenenberger, C. A. Surface morphology and mechanical properties of MDCK monolayers by atomic force microscopy. *J. Cell Sci.* **1994**, *107*(Pt 5), 1105–1114.

[105] Valberg, P. A.; Albertini, D. F. Cytoplasmic motions, rheology, and structure probed by a novel magnetic particle method. *J. Cell Biol.* **1985**, *101*, 130–140.

[106] Wang, N.; Butler, J. P.; Ingber, D. E. Mechanotransduction across the cell surface and through the cytoskeleton. *Science* **1993**, *260*, 1124–1127.

[107] Kole, T. P.; Tseng, Y.; Wirtz, D. Intracellular microrheology as a tool for the measurement of the local mechanical properties of live cells. *Methods Cell Biol.* **2004**, *78*, 45–64.

[108] Apgar, J.; Tseng, Y.; Fedorov, E.; Herwig, M. B.; Almo, S. C.; Wirtz, D. Multiple-particle tracking measurements of heterogeneities in solutions of actin filaments and actin bundles. *Biophys. J.* **2000**, *79*, 1095–1106.
[109] Xu, J.; Palmer, A.; Wirtz, D. Rheology and microrheology of semiflexible polymer solutions: Actin filament networks. *Macromolecules* **1998**, *31*, 6486–6492.
[110] Panorchan, P.; Lee, J. S. H.; Kole, T. P.; Tseng, Y.; Wirtz, D. Microrheology and ROCK signaling of human endothelial cells embedded in a 3-D matrix. *Biophys. J.* **2006**, *91*(9), 3499–3507.
[111] Zhou, X.; Rowe, R. G.; Hiraoka, N.; George, J. P.; Wirtz, D.; Mosher, D. F.; Virtanen, I.; Chernousov, M. A.; Weiss, S. J. Fibronectin fibrillogenesis regulates three-dimensional neovessel formation. *Genes Dev.* **2008**, *22*, 1231–1243.
[112] Flanagan, L. A.; Ju, Y. E.; Marg, B.; Osterfield, M.; Janmey, P. A. Neurite branching on deformable substrates. *Neuroreport* **2002**, *13*, 2411–2415.
[113] Tseng, Y.; Wirtz, D. Dendritic branching and homogenization of actin networks mediated by Arp2/3 complex. *Phys. Rev. Lett.* **2004**, *93*, 258104.
[114] Tseng, Y.; Fedorov, E.; McCaffery, J. M.; Almo, S. C.; Wirtz, D. Micromechanics and microstructure of actin filament networks in the presence of the actin-bundling protein human fascin: A comparison with a-actinin. *J. Mol. Biol.* **2001**, *310*, 351–366.
[115] Klein, M. G.; Shi, W.; Ramagopal, U.; Tseng, Y.; Wirtz, D.; Kovar, D. R.; Staiger, C. J.; Almo, S. C. Structure of the actin crosslinking core of fimbrin. *Structure* **2004**, *12*, 999–1013.
[116] Esue, O.; Carson, A. A.; Tseng, Y.; Wirtz, D. A direct interaction between actin and vimentin filaments mediated by the tail domain of vimentin. *J. Biol. Chem.* **2006**, *281*, 30393–30399.